(6) ACOUSTICALLY SCANNED OPTICAL IMAGING DEVICES

(9) Semiannual Report, No. 7

1 July — 31 December 1978

(12) 52

LEVEL II

Principal Investigator:

(10) G. S. Kino
(415) 497-0205

Sponsored by
Advanced Research Project Agency
ARPA Order No. 2778

(15) N00014-76-C-0129
Program Code Number: 4D10
Contract Period: 1 July 1975 - 30 September 1980
Amount of Contract: $504,302.00
Form Approved, Budget Bureau - No. 22R0293

Scientific Officer:

Dr. Max Yoder
Director, Electronic and
Solid State Sciences Program
Physical Sciences Division
Office of Naval Research
Department of the Navy
800 North Quincy Street
Arlington, Virginia 22217

(14) G. L. Report No. 2923

(11) February 1979

(12) 54 p.

Edward L. Ginzton Laboratory
W. W. Hansen Laboratories of Physics
Stanford University
Stanford, California

409 640

DISCLAIMER NOTICE

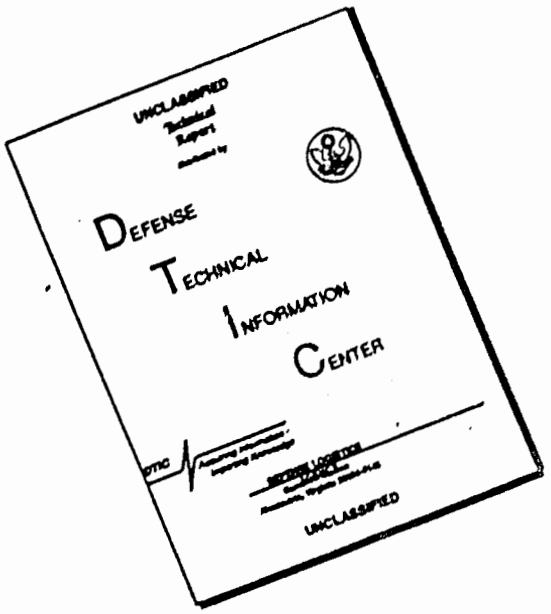

THIS DOCUMENT IS BEST QUALITY AVAILABLE. THE COPY FURNISHED TO DTIC CONTAINED A SIGNIFICANT NUMBER OF PAGES WHICH DO NOT REPRODUCE LEGIBLY.

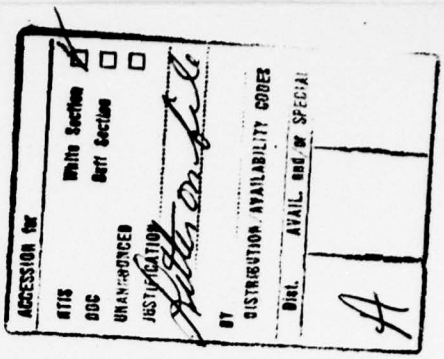

TABLE OF CONTENTS

I. MANAGEMENT REPORT

A. Summary

Our ZnO rf sputtering system has been tested more thoroughly in the last three months. We have succeeded in making high quality reproducible volume wave transducers with as good as and in some cases better characteristics than any we have made before. Deposition rates are a factor of six higher than in our previous system and a factor of two higher than the Japanese work. We believe, from our experience, that the deposition rate can be made still higher while at the same time obtaining better quality films. Experiments have been carried out depositing ZnO on gold, on SiO_2, on Si, and on quartz. All the layers look to be good quality. We have just begun to construct surface wave devices made with this technique. We anticipate that the results will be excellent and reproducible.

It was shown in the last Management Report that our ZnO on Si correlator can be operated in a new mode in which the signal reference is fixed in length but the amplitude and time of the unknown input signal can be varied. In this mode, the output of the device is highly linear with respect to variation of the time length of the input signal and of its amplitude. These are very important results as far as use of the device as a correlator is concerned. We have now taken these results further and shown that we can repeat an input signal several times and build up the amplitude of the stored wave by repeating the signal. Again, the results give us the maximum possible output obtainable with the device.

An important breakthrough has been to demonstrate that this device can be used to eliminate an interfering cw signal by operating it as an adaptive

filter. At the present time, our results indicate a 30 dB reduction in cw interference when both the cw signal and a p-n code are read into the device at the same time.

We have invented a new configuration to make the device an adaptive equalizer. We are presently testing out these concepts which are very simple in nature and which should make it possible for a device of this kind to adapt to an input signal with a few hundred iterations. No computer control is required because a feedback system is employed which should converge to its final equalization within 100 to 500 msec . We hope to have successful tests of this concept within the next few months.

Because of our heavy concentration on ZnO technology, and the use of the new sputtering system for this purpose, we have not constructed any complete surface wave devices during the last few months. Thus our work on GaAs has been proceeding slowly. We have improved our surface technology so that the quality of the surfaces is now better than it was before, and we have made excellent reproducible Schottky diodes with the high breakdown voltage that we observed earlier, but lower forward voltages for turn-on.

Our work on the edge bonded transducers was begun before we had realized that we might have a major breakthrough on the ZnO technology. Therefore, the edge bonded transducer is not as necessary as it was before. This is fortunate because we have encountered major technological difficulties associated with the lapping and grinding problem and associated with use of an interdigital transducer on the top surface rather than a true edge bonded transducer. The latter configuration tends to excite bulk waves strongly; the true edge bonded transducer, although an excellent transducer which we will pursue further, is extremely difficult to make. We have made some transducers which have poor efficiency but have very large bandwidths. We hope to improve its efficiency.

B. Research Program Plan

We intend to concentrate more fully on the ZnO on Si configuration because of the excellent prospects of our ZnO deposition system. The results always seem to be reproducible and always seem to be understandable. This is a major change. Therefore, we will be constructing ZnO on Si correlators using both Schottky diodes and p-n diodes for the purpose. At the same time, we will be proceeding with construction of GaAs convolvers using the same ZnO technology. We intend to test our new inverse filter equalizer and demonstrate that we can indeed make a programmable adaptive equalizer with a ZnO on Si monolithic correlator.

C. Major Accomplishments

Our ZnO magnetron discharge sputtering system appears to be very successful. All our results obtained so far are extremely encouraging. Our deposition rates are a factor of six higher than the earlier system and should reach a factor of ten before we are finished. These deposition rates are a factor of two to three times larger than is presently being employed by the Japanese.

D. Problems Encountered

Our work on GaAs and on other complete devices has slowed down because of our ZnO effort.

E. Fiscal Status

Total amount of contract	$504,302
Expenditures & commitments through 12/31/78	$338,207
Estimated funds required to complete work	$166,095
Estimated date of completion of work	30 September 1980

F. Action Required by ARPA/ONR

No specific action required.

II. TECHNICAL PROGRESS REPORT

I. INTRODUCTION

During the last six months, the research has taken a slightly different direction than that in the previous six months. This is because:

1. Zinc oxide on silicon technology appears to be on the verge of major improvements, leading to reliable, high quality fast depositions;
2. The ZnO on Si correlators appear to be directly capable of carrying out equalization and adaptive filtering of interfering signals, without external control by a computer for the adaption to take place.

For these reasons, we have concentrated more heavily on the development of the ZnO technology and on testing of already constructed correlators. At the same time, we have tried to arrive at very broadband transducers for use with both Si and GaAs convolvers and correlators.

A. Correlation and Inverse Filtering

A major breakthrough, which was described in part in the last progress report, was to demonstrate that the correlator can be used to filter out an interfering cw signal to which it adapts. Since the time of the last progress report, we showed that we could employ input correlation techniques to make a more precise adaptive filter. With this method we were able to obtain a 30 dB reduction in an interfering cw signal over the bandwidth of the device

(in this case 8 MHz). This work is described in an accompanying paper which was delivered at the 1978 Ultrasonics Symposium.

At the same time, we made a very complete demonstration of a new mode of operation in which relatively large signals could be used in the input storage mode, and the signals to read out the stored signal were larger than either of the input signals. This implies that the output reading system acts as a switch to turn the diode on or off, giving a destructive, but at the same time a very efficient, read out. The switch only turns on at a potential larger than that on the diode due to stored charge. This makes the device extremely efficient, relative to the original system. It also has the other major implication, for which we do not have a complete explanation, that if the reference signal is kept large in amplitude and fixed in time length, the output due to the input signal will vary linearly with the input signal amplitude and with the time of correlation. This linearity is observed over the complete dynamic range of the system, which at the moment is of the order of 35 dB because of spurious signals on the readout. This unexpected, completely linear behavior is extremely important, for it makes the device an ideal correlator. We have demonstrated the correlation times as long as 10 millisec . The results are described in the accompanying paper.

Based on this work, we have invented a feedback configuration which should enable the correlator to act as an equalizer to an arbitrary input signal. With this technique, we can send in an arbitrary input signal, specify the desired output, and by an iterative feedback technique, cause the correlator to adapt to produce the desired output. It is necessary to operate the device in this manner to be able to repeat the reference input signal many times and gradually build up weighting of the correlation-transversal filter.

Therefore, the last few months have been spent in demonstrating that we can build up a reference in this manner, and, in fact, can build up the weighting gradually over many iterations. We have shown that indeed we can do this extremely well. For instance, we can store a Barker Code by repeating it many times. We are now at the point of testing the inverse filter; we hope to have demonstrations of such an equalizer inverse filter in the near future.

B. ZnO Technology

At the last Ultrasonics Symposium, Shiosaki et al. delivered an impressive paper which described the latest Japanese ZnO technology and demonstrated that ZnO on glass devices could be made routinely at high speed and extremely reproducibly. Evidently such devices are now being produced in production quantities for TV IF filters and watch crystals. The basic technique he described involved the use of a magnetron sputtering system which we were already in the process of building. We therefore decided to put a great deal of effort to perfecting our own system, which we believe has advantages over the Japanese one, and which we believe will be of great importance not only to our own convolver correlator work, but also to the technological capabilities of this country.

As we have described earlier, the problem has always been reproducibility of the ZnO films. Typically, we could and have made highly reproducible films on top of a gold film. But the films obtained on other substrates were variable. The reason for this is the substrate heating caused by electron bombardment from the plasma discharge, the production of traps in the ZnO due to the electron bombardment, and the fact that the surface temperature was therefore very dependent on the plasma discharge conditions,

the thermal conductivity of the substrate, and the contact between the substrate and the substrate holder.

The magnetron discharge has the great advantage that most of this bombardment should not take place, and therefore the substrate temperature can be far better controlled. In addition, as distinct from the Japanese, we have a pure zinc source, and we can obtain much higher rates of bombardment of the target because it can be cooled easily.

Our initial results are extremely encouraging. Every run we have had has given good quality ZnO; the only exceptions are always explainable. This was not usually the case before. All tests that we have carried out indicate that we have obtained high quality films, so we expect to be making high quality reproducible devices by this technique.

The considerable attention that we have paid to this technology has meant that we have not been producing devices during the last few months. But we believe that this temporary halt in producing devices is more than worthwhile because of the ultimate capability we should have for this purpose.

C. Edge Bonded Transducers

We have also been developing other kinds of broadband transducers. Initial effort on this edge bonded transducer was due to the fact that we did not believe we could easily make broadband ZnO transducers. Now because of the improvement of the ZnO technology, it may not be necessary to develop alternative transducers, for we can deposit arbitrarily thick films at will. Thus, we will carry out a few runs on the edge bonded transducer concept, but we will probably taper off this effort.

D. GaAs Technology

The GaAs technology has also been going rather slowly because of the concentration on the ZnO technology. So as the ZnO station was not available for routine production of surface wave transducers, we have not been able to construct complete devices in the last few months. On the other hand, we have improved our surface preparation techniques so as to obtain far more highly reproducible surfaces and, in particular, more reproducible Schottky diodes.

E. Schottky Diodes

At the same time, although it was not described in this report, we have been constructing a secondary system for making Schottky diodes in silicon using the platinum silicide technique. Some work was done in this direction, approximately two years ago, by our group at Stanford. We are now interested in making Schottky diode on silicon devices because of the fast input storage times.

II. DEVELOPMENT OF ZnO TECHNOLOGY

In our previous report, we described the design of a new ZnO sputtering system. The system has a planar magnetron discharge sputtering head used to sputter zinc in an oxygen atmosphere and form zinc oxide on the substrates of interest. The sputtering system has been built, and preliminary results indicate that well oriented films and high sputtering rates are possible.

We are carrying out a series of sputtering runs on various substrates, and under various deposition conditions, in order to determine the optimum conditions of growth of ZnO films. The substrates of interest are: oriented gold, quartz, silicon, and gallium arsenide. The quality of the sputtered films is evaluated using the following techniques:

- X-ray diffraction
- X-ray microprobe
- Scanning electron microscopy: surface and fracture edge
- Reflection electron diffraction
- Acoustic measurements

Typically, whenever a ZnO run is made, a bulk wave transducer is made on a sapphire delay line, and its round trip insertion loss is measured. Later, the X-ray and electron microscopy work is done on other samples made in the same run. The results of all the tests are then used to change the deposition parameters of the next run.

On the basis of our previous experience in the field and T. Barbee's preliminary results at the Center for Materials Research, we used the following conditions as a starting point:

oxygen pressure	7 microns
substrate temperature	300° C
rf power	1000 watts
target to substrate distance	7.5 cm
sputtering rate obtained	6 μm/hour

The tuned round trip insertion loss of the ZnO/sapphire delay line was typically 9 dBs at a center frequency of 1 GHz. This indicates that a good quality ZnO film is obtained, as good as the best films obtained in our previous sputtering station for which k_t^2 was 90% of its theoretical value. In this case, however, the sputtering rate was 6 μm/hour , approximately six times as fast as before. The sputtering rate obtained is twice as high as already reported in the literature; this is due to the fact that we use a zinc target that is in much better thermal contact with the cooling water. Hence, more rf power can be applied to the target.

The X-ray microprobe results indicate that zinc and oxygen are the only elements present in the film. This confirms our prediction that higher purity ZnO can be obtained using a pure zinc target, instead of a ZnO target. The result also indicates that the vacuum station we built is very clean. Another result of the X-ray microprobe is that the ZnO films were slightly oxygen rich: 60-40: O-Zn. We believe that the films are indeed oxygen rich, but by less than the percentage indicated because of the large correction needed in the calculation of the concentration of the elements (195%). The oxygen richness can be corrected either by increasing the power, or by decreasing the oxygen pressure. Thus, it should be possible to sputter even better films than already obtained.

The X-ray diffraction results indicate a strong orientation of the films in the (0002) direction as expected. The quality of the films on gold and quartz were very good. The quality of the films on SiO_2/Si was not as good. However, a peak corresponding to a lattice spacing of 6 Å was observed on the diffractometer trace for the ZnO/SiO_2/Si case. As we do not know of any planes with such a large d spacing in any of the materials tested, we suspect an error of measurement in this case, and the X-ray test is being repeated.

Figs. 1a, 1b, 2a, and 2b show the results of the S.E.M. of the ZnO films on F.Q. and SiO_2/Si. Figs. 1a and 1b are S.E.M. of the surface of the ZnO films; both figures indicate that the films are very smooth and show no indications of relieved areas exhibiting small bumps as in our previous films. This is an indication that indeed we are depositing better films than in our previous ZnO station. Figs. 1b and 2b are S.E.M. of the fracture edge of the ZnO films. Again, these films show the preferred orientation of growth normal to the substrate in the 0002 direction. This result is, of course, confirmed by the X-ray diffractometer data.

We have tried one run with the same conditions as before except for the rf power which was increased to 1250 watts. A sputtering rate of 7 μm/hour was obtained, and the tuned round trip insertion loss of the transducer was 6.5 dBs. This latter result is so much better than our previous runs (9 dBs with k_T^2 = 90% of theoretical) that we find it difficult to explain why it is so good. Obviously, increasing the power improved the quality of the film as expected. We are presently carrying out the rest of the evaluation step on the various films obtained.

The one problem that we have met so far in this station is that of knowing the surface temperature of the substrates. This knowledge is important because a stainless steel holder is being used, and the indication of a thermocouple can be very different from the real temperature of the substrate because of the larger thermal gradients that can exist in stainless steel. We are presently making thin film resistors that we plan to use to monitor the temperature of the surface on which the ZnO is being deposited.

III. EXPERIMENTS WITH THE STORAGE CORRELATOR

A. Introduction

It has been our aim to arrive at a technique for employing the storage correlator as an adaptive equalizer or inverse filter. In the last progress report, we described one version of this adaptive filter which we employed to remove an interfering cw signal. By working in an input correlation mode, we have been able to obtain as much as 30 dBs reduction of an interfering cw signal introduced into the device at the same time as a PN code. This work is an extension of the earlier work we described in the last progress report and is dealt with in an accompanying paper which was delivered at the 1978 Ultrasonics Symposium.

More recently, we have been able to arrive at a new design to program the device as an inverse filter or equalizer and have been pursuing techniques to allow us to accomplish this purpose. The basic device configuration required for the inverse filter is shown in Fig. 3. As will be seen from the schematic, the method is relatively simple. It requires a test signal $X(t)$ to be inserted into the device repetitively. Suppose the weighting of the device along its length is $w(z)$. Then, when the pip signal is inserted into it, an output will be obtained of the form:

$$Y(t) = \int X(t - z/v)\, w(z)\, dz \qquad (1)$$

where z is the distance along the device and v is the acoustic velocity. The required signal $-D(t)$ is fed into an amplifier along with $Y(t)$ so that the error between the output and the required signal is found. This is:

$$\varepsilon(t) = Y(t) - D(t) \qquad (2)$$

The switch shown is then moved to its second position. The error signal passes through a delay line back into the device while at the same time, the test signal $X(t)$ is re-inserted into the device. The correlation between the test signal and $\varepsilon(t)$ is therefore obtained in the device and serves to up-date the weighting of the storage correlator. By this means, the device iterates several times until a final weighting is such as to make $Y(t) \to D(t)$. It can be shown that in fact this process constructs a Wiener filter. After the device is set, the weighting remains essentially constant for the storage time of the device, and it can therefore be used as an equalizer for any signal entering it.

Very similar configurations can also be employed to remove interfering signals or to eliminate noise. As each iteration around the device takes of the order of 6 μs , it will be seen that the device can rapidly converge on a final weighting. This compares very favorably with the similar process, when carried out with a computer or microprocessor, for our iteration times are of the order of a few microseconds where the iteration times in a computer might be as much as several seconds. The storage correlator appears to be ideally suited to this purpose because it carries out all of the processes required in almost the optimum configuration.

It will be seen that a basic requirement of the technique is to be able to insert a signal and build up the amplitude of the storage progressively with time. Therefore, as a first step, it was necessary to determine if we could indeed do this. We had already shown that by working in the input correlation mode, it is possible to build up a correlation peak. This is near to what was required; however, we felt that before proceeding with experiments on the inverse filter, it was necessary to demonstrate that by reading in a signal repetitively, we could build a stored signal up to its final amplitude after many cycles of input signal and finally correlate it with later signals, if need be.

Therefore, two main experiments have been tried in which cw pulsed signals and Barker Codes were stored repeatedly and correlated with later signals.

B. CW Correlation

A schematic of the set-up employed is shown in Fig. 4. An rf pulse is generated periodically by the Rep. Rate Generator which is gated in turn by the mode Control Generator which defines two modes separated in time, the store mode and the read-out mode. The period of this mode is 70 msec ,

which allows enough time for the diodes in the storage correlator to discharge. The time-length of the store mode can be set at will to nearly 70 msec , thus varying the number of stored acoustic signals. On the top-plate, we apply a train of write-in pulses, triggered by the Rep. Rate Generator and synchronized with the acoustic signal. The pulse width can be changed at will, as well as the delay of these pulses, relative to the acoustic signal. Finally, a read-out pulse is applied to the top plate; this signal is generated from the delayed falling edge of the store mode pulse and also controls the output gate. The same rf source at 120 MHz is used to generate the carrier signal. Level of applied signals as shown were taken from Fig. 4 where it was shown that these are optimum values.

C. Results of CW Experiment and Comments

1. Pulse Width of Write-in Signals as Function of N (Number of Input Stored Signals)

The function is hyperbolic as we can see from Fig. 5. The correlation peak is kept constant during the pulse width decrease process. The results indicate that it is the total charge read into the system which controls the storage phenomenon.

2. Correlation Peak Versus Number of Integrating Pulses

The function in Fig. 6 is non-linear and saturated very rapidly as an exponential, as we increase the number of stored signals. This is in complete agreement with Ref. 1. The correlation peak is larger in our case by 6 dB as the acoustic power input was 16 dBm instead of the 10 dBm was in (1). The signal duration or integration time is the number of acoustic stored pulses times the width of the write-in pulse (1 μsec). Saturation at about 80% of the final value occurs after 20 μsecs of integration time.

The optimum choice for the number of integrating pulses in a cw correlation system is therefore determined to be between 20 and 100.

3. Linearity of Acoustic Port (Input Dynamic Range)

Very good linearity has been obtained over a 25 dB dynamic range as the acoustic power fed to the acoustic port was increased. Good linearity (within 1 dB of the linear curve) is obtained over a range of 30 dB.

We conclude that the dynamic range is 30 dB . The limiting factor for the low signal is the spurious level which is above the noise level by 10 to 15 dB . Thus, as we reduce the spurious signals we should be able to increase the dynamic range. The maximum input power to the transducer determines the maximum input signal.

4. Linearity of Top-Plate

Excellent linearity was obtained with the read-out signal power when decreased by more than 40 dB , while the write-in signal was held constant. In this case the limiting factor is the noise of the system. There is no problem of spurious signals because these are generated by high level read-out signals.

D. Barker Code Correlation

1. Conditions of Experiment

We used the same set-up as described in Fig. 4, except that now two Barker Code generators are inserted in the signal path of the acoustic port, and the delayed Barker Code version is applied at the top-plate to read out the correlation signal. The storage correlator with a time bandwidth capability of 24 (8 MHz bandwidth and 3 μsec storage length) allows us to correlate and store Barker Codes up to 13 bits. So we made our

experiments with a 5-bit, 7-bit, and 13-bit Barker Code. The parameters used were:

Length of Barker Code	3 μsec
RF Frequency	120 MHz
Acoustic level	4 v.p.t.p/50Ω
Write-in and Read-out signal	8 v.p.t.p/50Ω
Interval between signals stored	6 μsec

2. Results Obtained

a. The input dynamic range was measured as 30 to 35 dB which complies with the cw experiment.

b. The larger the number of N for a given correlation peak output, the narrower the write-in pulse can be made; this relationship is hyperbolic as in the cw case.

c. The output dynamic range is the output correlation peak as function of the integration time (or number of store signals). We can see from Fig. 7 that this range is about 20 dB , which compares well with the input correlation mode experiment [see Fig. 6 in (1)]. Storing one single Barker Code produces a correlation peak of 60 mV; saturation is achieved after 320 pulses (or 320 μsec integration time for a 1 μsec write-in pulse) producing about 0.5v.

The curve shown in Fig. 7 is fairly linear; this is due to a lower top plate voltage in this case than in the cw case. We also need a larger number of integrating pulses than in the cw case, for the same reason.

The advantage of the repetitive store method is that we can always achieve the maximum correlation peak by increasing the number of the integrating pulses up to a theoretical value of 23,000 (3 μsec pulses divided into

maximum allowable time for storing which is 70 msec). In almost all cases, saturation will occur far before this level.

d. The sidelobe level was close to the optimum as will be seen from Table I.

TABLE I: Barker Code Sidelobe Levels

Length of Barker Code	Theoretical Value of Sidelobe Level	Experimental Value Obtained
5-bit	14 dB	14 dB
7-bit	17 dB	16 dB
13-bit	22.2 dB	20 dB

Fig. 8 shows a 13-bit Barker Code correlation. Notice that the output signal is well above noise.

e. The storage time defined as the time when the output correlation drops by 3 dB was measured and found as 58 msec.

E. Conclusion

The repetitive store mode offers a highly efficient way to store and correlate pulsed signals, especially short signals such as Barker or Huffman Codes, making use of the pulse compression capability of the device. The optimum correlation peak can be obtained by increasing the time of integration up to the limit of the discharge of the diodes. The method opens up new horizons in signal processing, as many successive complex operations of convolutions and correlations can be made during the store mode time.

As we have discussed, an important application of this new method is to design an adaptive filter in which the input signal will be trained with another signal by using the L.M.S. algorithm. The store mode will

allow enough time for the filter to adapt to the training signal, and the weighting function of the device will be updated after each iteration created by one single pulse. Each iteration can last in theory as short as 3 μsec (the acoustic storage time), and so the adaption time should be only 100 - 500 μsec . Our next step will be to use this method to construct an adaptive Wiener filter.

F. References

1. H. C. Tuan, P. M. Grant, and G. S. Kino, "Theory and Application of Zinc-Oxide-on-Silicon Monolithic Storage Correlators," presented at 1978 Ultrasonics Symposium, September 1978, G. S. Report 2872.

IV. GaAs CONVOLVERS AND CORRELATORS

The aim of our GaAs work is to fabricate both monolithic convolvers and storage correlators. Initially we intend to demonstrate working devices using ZnO as the transducer material. A new magnetron discharge ZnO sputtering station has been built. This station is believed to be capable of depositing ZnO film of higher quality at a faster rate. Test runs have been carried out to search for optimum deposition conditions, and preliminary experimental results are extremely encouraging. Since some of the electronic equipment on the old rf diode sputtering station has been disconnected to be used on the new station, we have not been able to use the old station to fabricate GaAs devices. Judging from the good results we have obtained, the new station should become available to us very soon.

Because of the unavailability of the ZnO station, or for that matter the edge bonded transducers described in Section V, we have concentrated

on improving our Schottky diode technology. There were two problems with our Schottky diodes in the past. The first is that the turn-on voltage of the diodes could be 2 - 5 volts, much larger than the theoretically predicted 0.3 - 0.4 volts. The second is that we could not obtain consistently a mirror-like GaAs surface after the etching and cleaning steps required in the fabrication process. The result of this is that the reverse breakdown voltage and the reverse leakage current of the diode varies considerably from run to run.

The first problem is believed to be caused by the non-ohmic contact on the back side of the GaAs. We have investigated this problem by depositing different combinations of metal films on the back side of the GaAs and varying the annealing temperature required. Our most recent recipe is 4000 Å Indium/4000 Å Gold and an annealing temperature of 275° C - 300° C. Fig. 9 shows the I-V characteristics of a diode with such a back side contact. The turn-on voltage is about 0.35 volts. The breakdown voltage is about 125 volts. The detailed I-V measurement reveals that a series contact resistance still exists. We believe this series resistance can essentially be eliminated by being more careful with the annealing process. Instead of annealing the samples in a controlled environment (like forming gas), we have been annealing them on a hot plate in the air environment. Presently, a small furnace for this purpose is being set up in the laboratory.

The second problem, we have found out recently, is caused by the etching solution used to remove the first 1 - 2 μ of the GaAs surface. This etching step is necessary because the first 1 - 2 μ of the surface is usually more heavily doped than the rest of the epi-layer as a result of the epitaxial growth. The etching solution we have used in the past is

10 H_2O : 1 H_2SO_4 : 1 H_2O_2 . Even with extreme care in mixing and stirring the etching solution, good consistent surface conditions were difficult to obtain. The surfaces look cloudy on many of the samples. Recently, we have changed the etching solution to 5 H_2SO_4 : 1 H_2O_2 : 1 H_2O . The result is very satisfactory. Mirror-like surfaces can be obtained reproducibly with much less care. With such high quality GaAs surfaces, we believe a diode array with good performance can be fabricated.

In the next six months, we will make improved GaAs convolvers using the non-linear conductance effect of the Schottky diodes, as we have discussed in our last progress report. Because of the improved etching technique, we are quite optimistic about fabricating the first monolithic GaAs storage correlator using the diode array structure.

V. EDGE-BONDED SAW TRANSDUCER

We have described in our last progress report the principle of operation of the edge-bonded transducer, the structure of which is shown schematically in Fig. 10a. Our preliminary experimental work on another contract has indicated that there are three drawbacks associated with the fabrication of this transducer structure at high frequencies:

1. The structure requires the deposition of metal electrodes on the ends of the device. Since the mask aligner in our laboratory was designed to handle planar samples typically 10 - 20 mils thick, photolithography presents a fabrication problem for our structure where the sample is usually 3 cm long or more;
2. The electrode metallization tends to extend over the edge of the PSN and become electronically shorted to the indium bonding layer. The situation worsens at higher frequencies because the PSN is thinner;

3. For a desired center frequency of 100 MHz, the PSN has to be polished to about 16 μ thick. Since it is extremely difficult to handle PSN samples at this thickness, the normal procedure is to bond a much thicker PSN piece to the substrate and lap it down afterwards. A second lapping process is also needed to level the PSN with the top surface of the substrate. Because of the stress involved in the two lapping steps, the thin PSN sometimes cracks.

To overcome these difficulties, we have proposed edge-bonded transducers with two different configurations. The basic idea is to indium-bond thick pieces (1 - 2 mm) of PSN to the ends of the substrate and fabricate transducer electrodes on the top surface of the PSN. The photolithography process involves only a planar structure and, therefore, it is compatible with existing alignment facilities and conventional planar technology. As thick PSN pieces can stand the lapping process, it is far easier to level the top surface.

Fig. 10b shows the first new electrode configuration proposed. An electrode $\lambda/4$ wide is laid on the PSN surface, separated from the indium-bond interface by a gap $\lambda/8$ thick. From symmetry consideration, the electric field distribution in the PSN with V volts applied on the electrode would be identical to that of a structure when the shorting plane at the bonding interface is removed, the substrate is replaced by PSN, and an identical interdigital electrode at a potential $-V$ is placed $\lambda/8$ away from the interface. For this reason, we call this structure a half-finger-pair transducer structure. Its principle of operation is similar to that of an interdigital transducer (IDT). The acoustic Q of the transducer, which is determined by the number of finger pairs of the IDT, is small. The reactive impedance of the electrodes, which is mainly determined by the static capacitance of the electrode, remains at a manageable level ($\sim$ 150 Ω at 100 MHz

or ~ 300 Ω at 50 MHz), thanks to the high dielectric constant of the PSN (~ 700). The electrical Q of the transducer is equal to $1/\omega_0 C(50 + R_a)$ when R_a and C are the radiation resistance and static capacitance of the transducer, respectively. Taking both the electrical Q and the acoustic Q into consideration, our rough estimate is that we should be able to get 40 - 50% bandwidth at a center frequency of 100 MHz.

In spite of the high dielectric constant of PSN, the reactive impedance of the transducer is still on the high side to make untuned operation less than optimal. One other potential disadvantage is the loss of efficiency because power is radiated into bulk waves. The obvious solution to these problems is to use an IDT structure having more than one finger pair, bearing in mind that the number of finger pairs should be properly chosen to achieve the desired acoustic bandwidth.

Since ~ 40% bandwidth is acceptable to us at the present time, we chose to employ the 2-finger-pair transducer structure, as shown in Fig. 10c. Assuming a dielectric constant of 700 and $\Delta v/v \simeq 0.02$, the radiation resistance and the reactive impedance of the IDT are estimated to be 15 Ω and 125 Ω, respectively. The untuned loss due to electrical mismatch at these impedance levels is ~ 8.5 dB per transducer.

We have fabricated transducers with both half-finger-pair and 2-finger-pair structures. PYREX glass was used initially as the substrate material because the composite structure of PSN/PYREX is easier to polish. Fig. 11 shows the indium bond in detail, and it can be seen that the bond is extremely uniform. We have successfully made two half-finger-pair transducers on the same substrate, one at each end. The center frequency of the transducer is designed to be approximately 50 MHz. Fig. 12 shows the impulse response of this delay line. The large bandwidth of the transducer is demonstrated by the one-and-half-cycle impulse response. The untuned rf tone-burst

measurement gives the 3 dB response from 35 MHz to 70 MHz . The larger-than-expected 70% bandwidth is probably due to the parasitic capacitance of the BNC connectors. The untuned terminal-to-terminal insertion loss is 47 dB at midband. The insertion loss drops to 32 dB when the transducers are tuned with inductors. Taking into account the series resistance of the transducer electrode, the insertion loss of 32 dB implies a radiation resistance of approximately 1 Ω . This is considerably lower than we had estimated.

Fig. 13 shows the Smith-Chart display of the input impedance of a 2-finger-pair 100 MHz IDT fabricated on PSN. The transducer is tuned so that the impedance near the center frequency can be displayed more clearly. Assuming a series electrode resistance of 10 - 15 Ω , both the real and the imaginary impedance of the transducer are close to what we would have expected. We therefore assumed that the IDT is working properly. Unfortunately, we had only one good transducer on this delay line and cannot measure the terminal-to-terminal insertion loss. We have fabricated more indium-bonded PSN/PYREX delay lines, having 2-finger-pair IDTs on both ends of the delay lines. For reasons not understood presently, we cannot reproduce the result shown in Fig. 13. The reactive impedances of these IDTs are always higher than that of the IDT displayed in Fig. 13. The tuned terminal-to-terminal loss is 35 - 45 dB for most of the delay lines tested. Again, this indicates that the surface wave radiation resistance is considerably lower than we expected.

We believe the reason for the small radiation resistance is that the PSN ceramics had been depoled during the fabrication process. This is conceivable considering that the fabrication process does involve sputter etching and sputtering of metal films, both requiring the bombardment of the PSN surface by energized particles. It should the pointed out that only

the surface layer (20 - 30 μ at 100 MHz) of the PSN is acoustically active with the IDT structure and any depoling due to the surface bombardment is going to have a large effect on the performance of the transducer. At the present time, we are taking steps to investigate and improve the fabrication process. This includes finding new ways to deposit the metal electrode, avoiding any sputtering steps.

FIGURE LEGENDS

1a. 1800X S.E.M. surface of $ZnO/SiO_2/Si$

1b. 5000X S.E.M. fracture edge of $ZnO/SiO_2/Si$

2a. 1000X S.E.M. surface of ZnO/F.Q.

2b. 5800X S.E.M. fracture edge of ZnO/F.Q.

3. Schematic of basic device configuration required for the inverse filter

4. Schematic drawing of cw correlation experiment

5. Pulse width of write-in pulse versus number of integrating pulses

6. Correlation peak as function of number of pulses

7. 13-bit Barker Code and stored charge pattern

8. Output dynamic range

9. I-V characteristics of a Schottky diode on GaAs (Vertical: 0.05 mA/div)

10a. Schematic of principle of operation of edge-bonded transducer

10b. Schematic of first new electrode configuration proposed

10c. Schematic of 2-finger-pair transducer structure

11. Indium bond between PYREX and PSN (400X)

12. Impulse response of the half-finger-pair edge-bonded transducer

13. Smith-Chart display of the input impedance of a tuned 2-finger-pair edge-bonded transducer

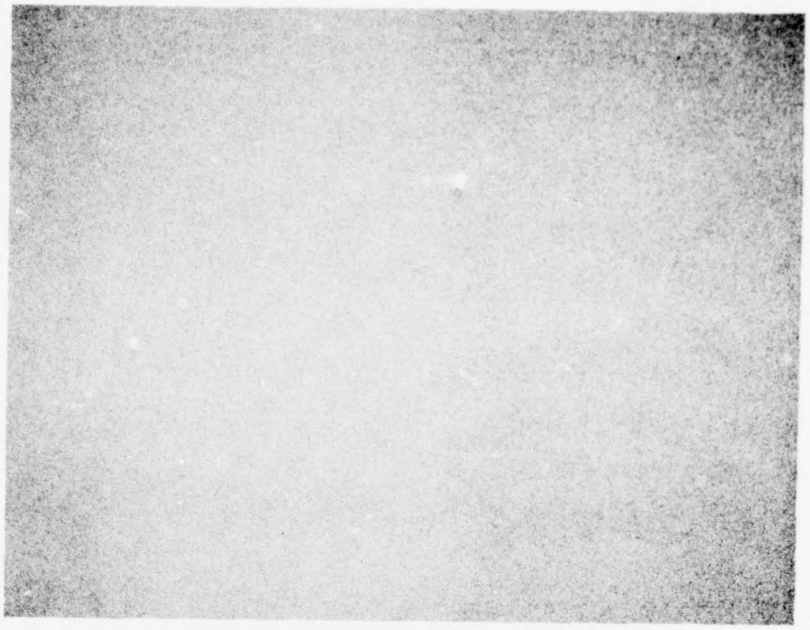

Fig. 1a

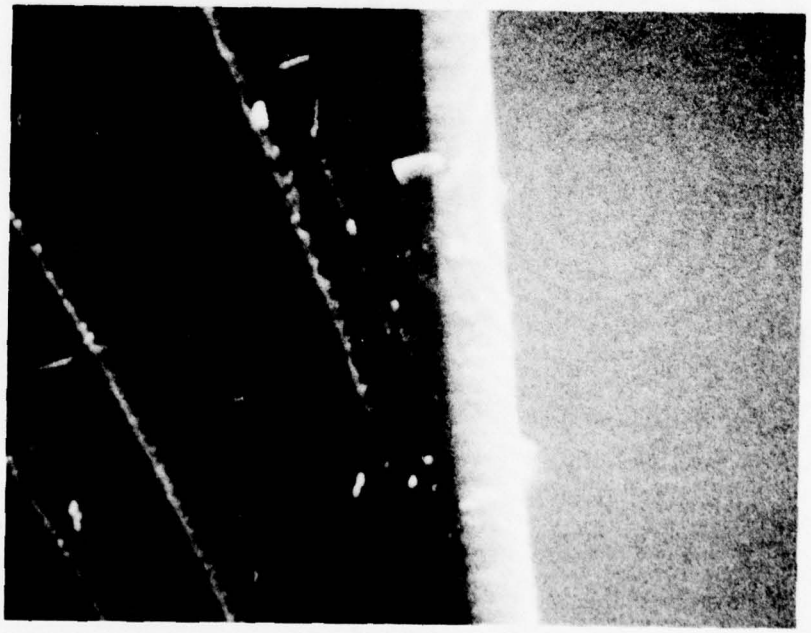

Fig. 1b

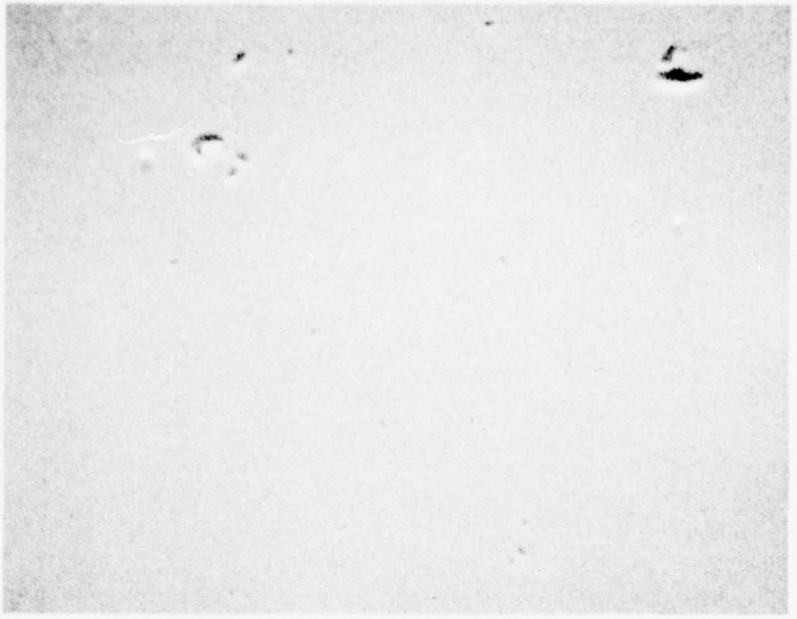

Fig. 2a

Fig. 2b

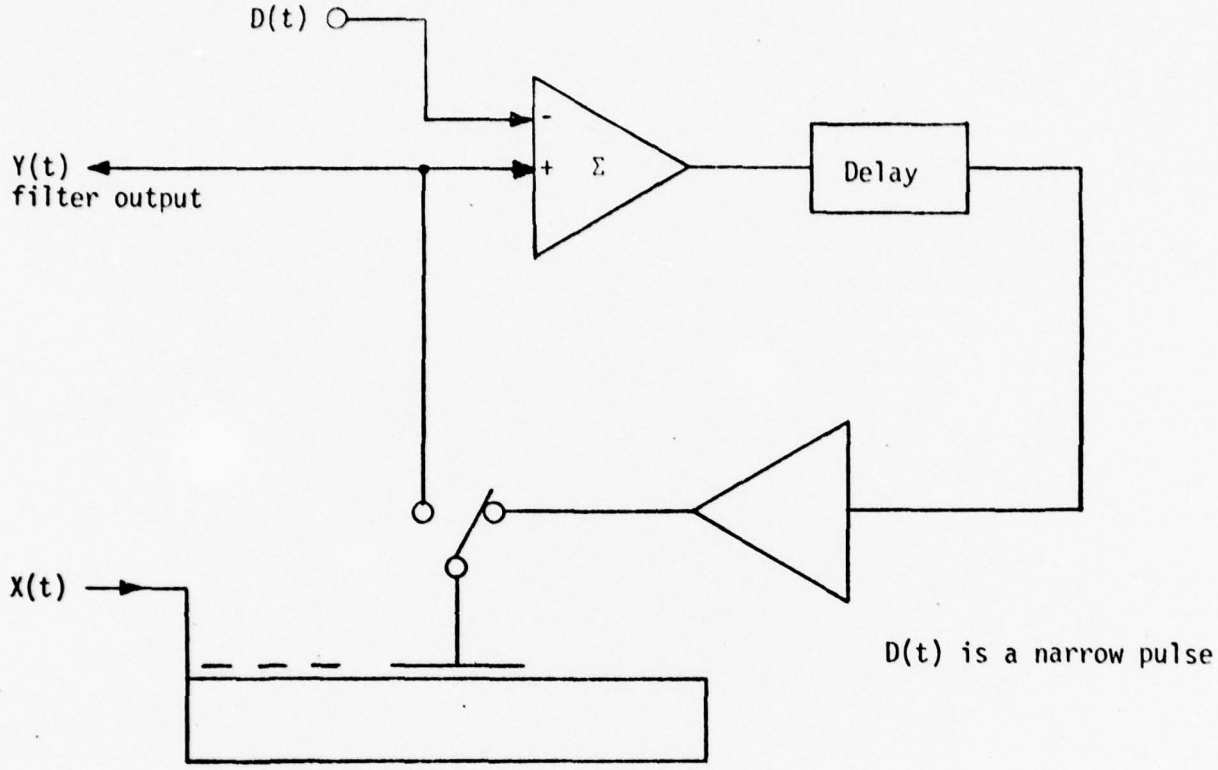

Fig. 3

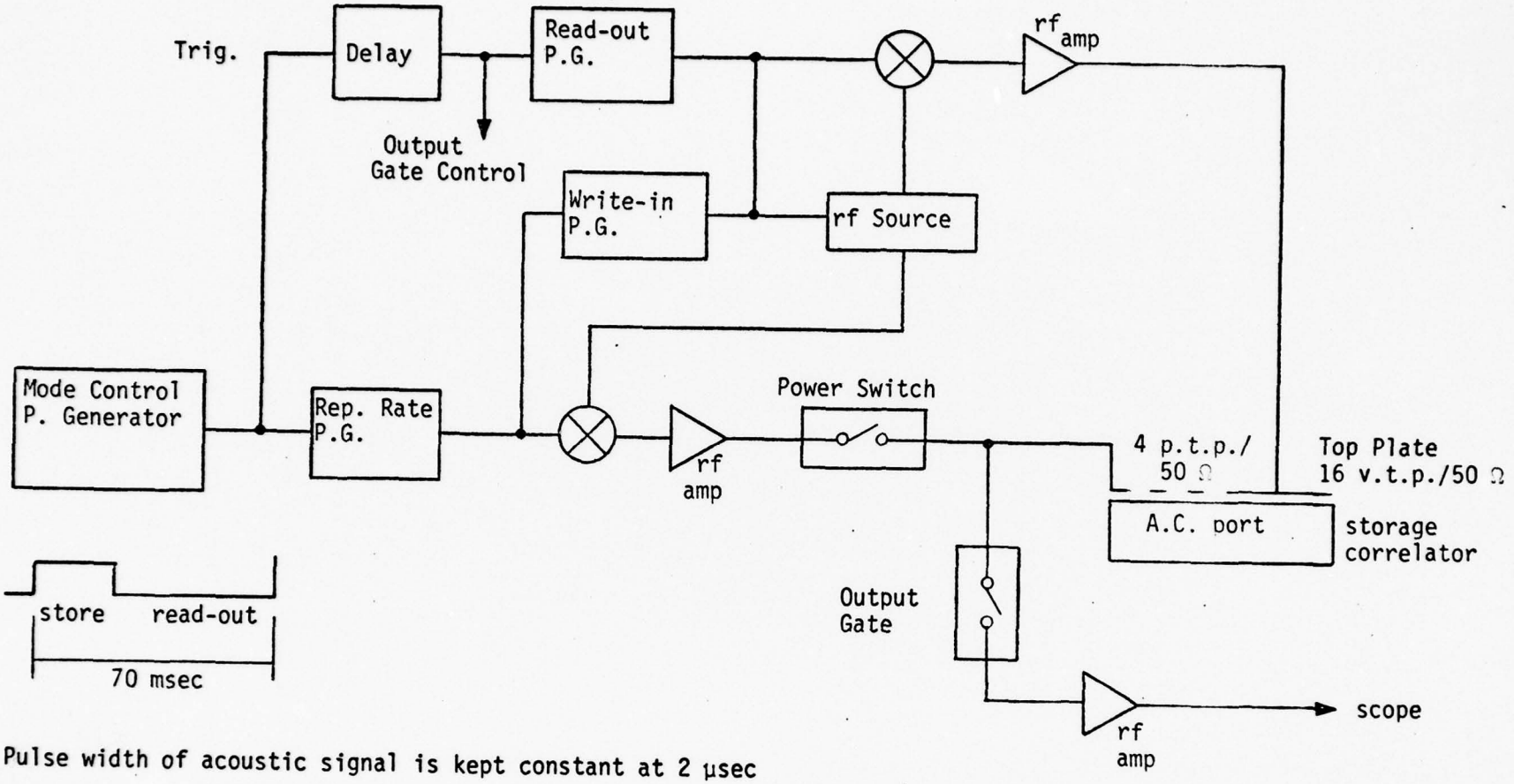

Pulse width of acoustic signal is kept constant at 2 μsec

Fig. 4

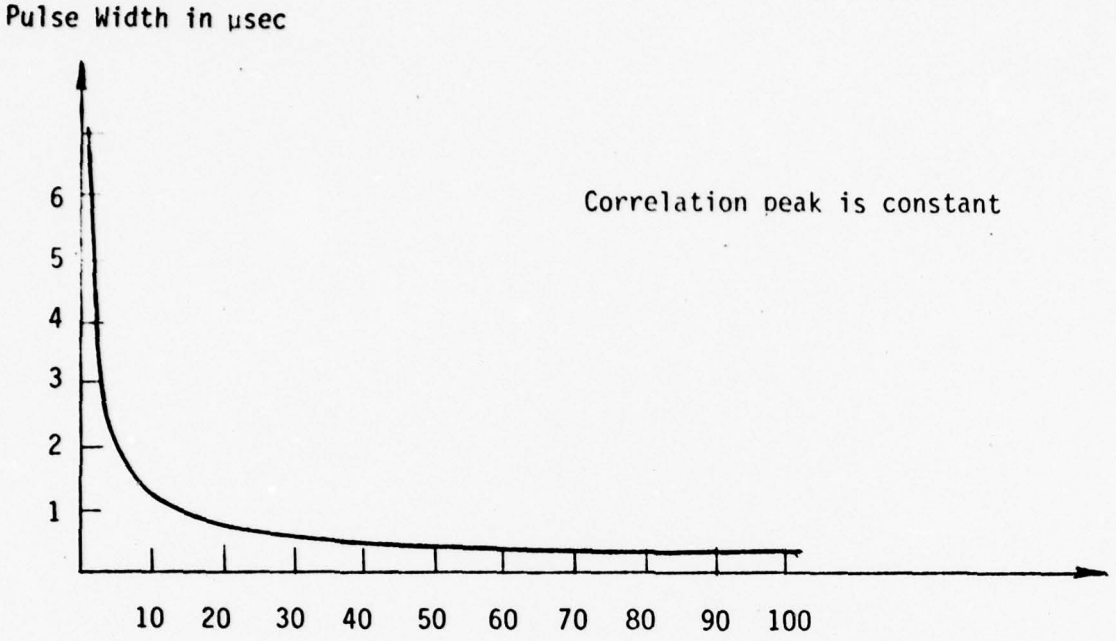
Pulse Width in μsec
6
5
4
3
2
1
Correlation peak is constant
10 20 30 40 50 60 70 80 90 100

Fig. 5

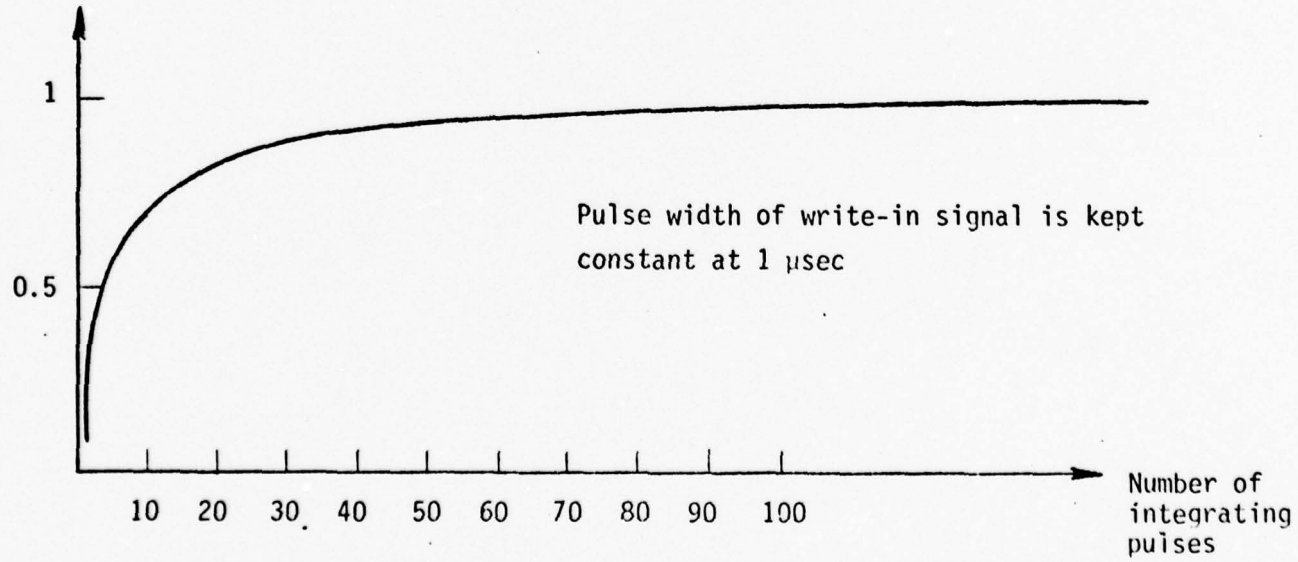
1
0.5
Pulse width of write-in signal is kept constant at 1 μsec
10 20 30 40 50 60 70 80 90 100
Number of integrating puises

Fig. 6

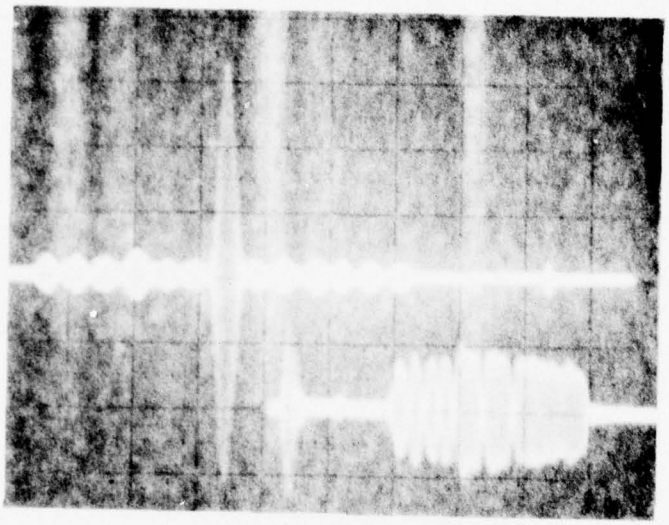

Fig. 7

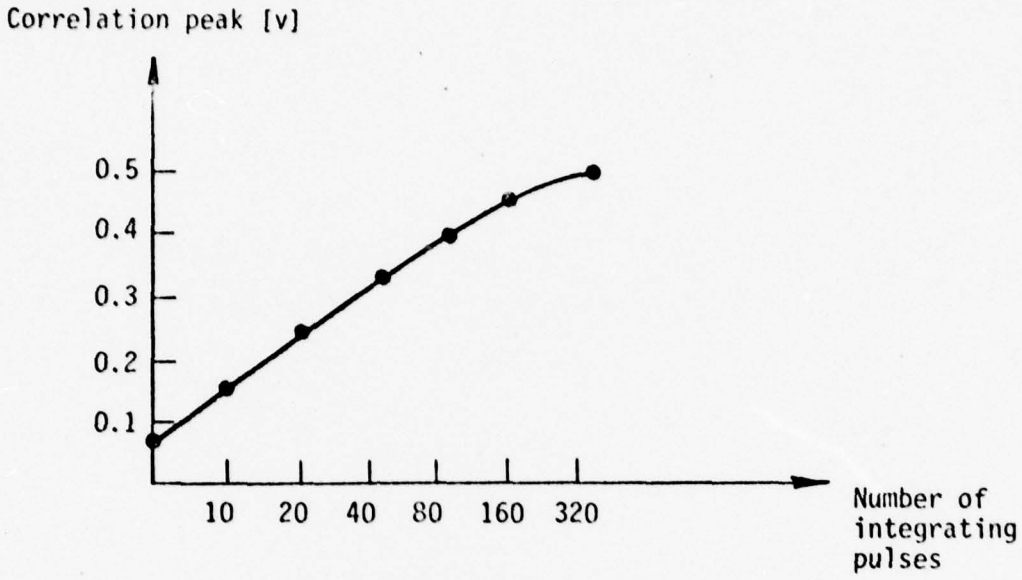
Correlation peak [v]
0.5
0.4
0.3
0.2
0.1
10
20
40
80
160
320
Number of integrating pulses

Fig. 8

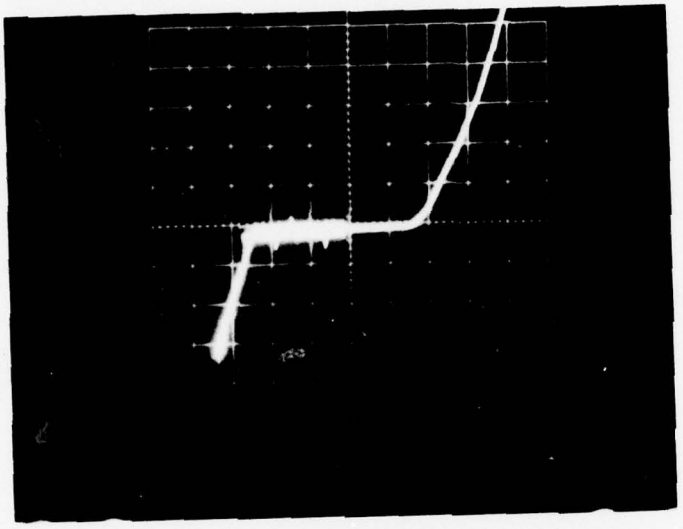

Reverse ←→ Forward
50 volt/div 0.2 volt/div

Fig. 9

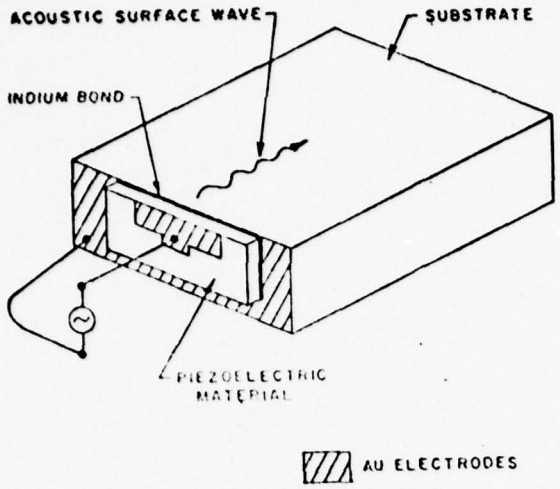

Fig. 10a

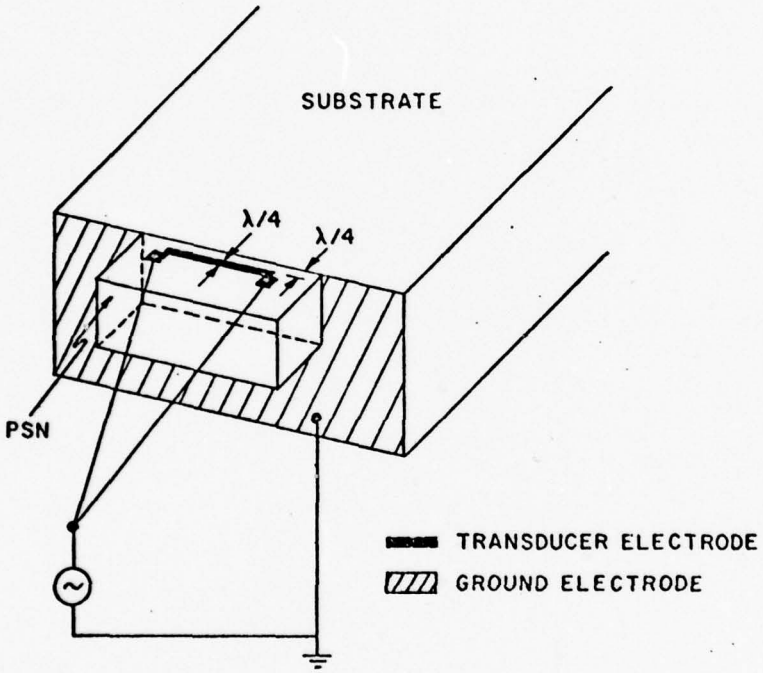

Fig. 10b

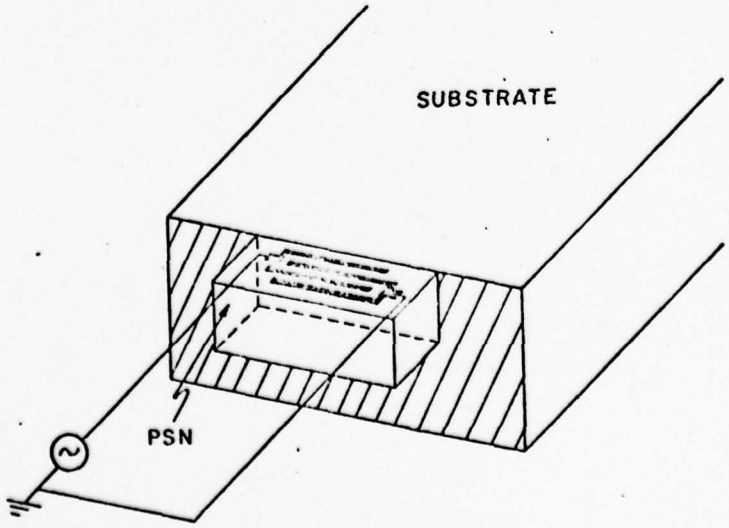

Fig. 10c

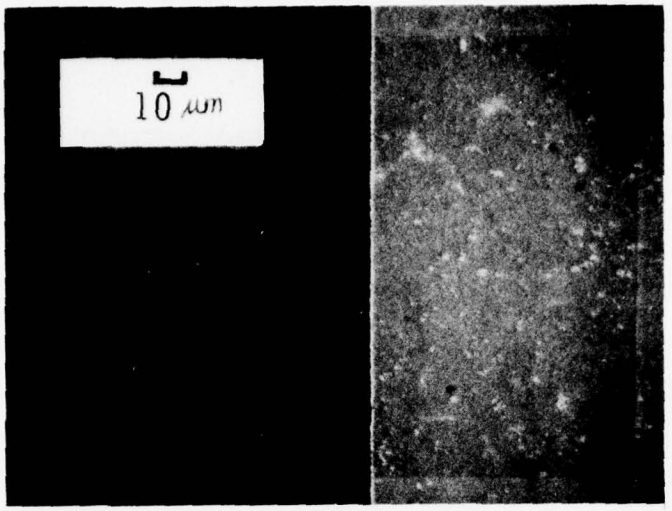

PYREX INDIUM BOND PSN

FIG. 11

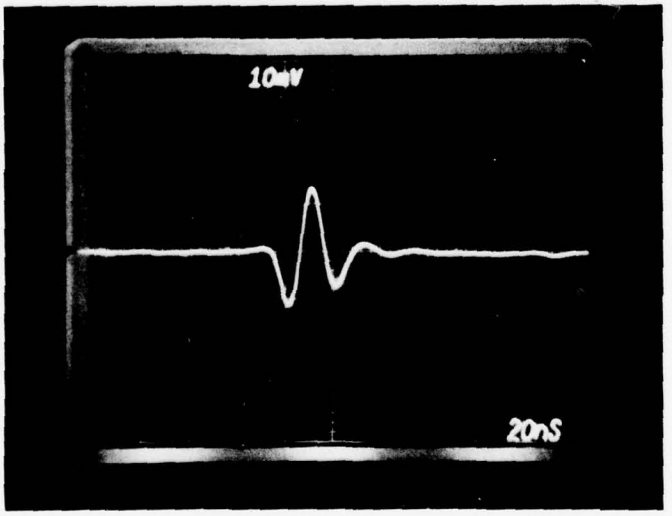

FIG. 12

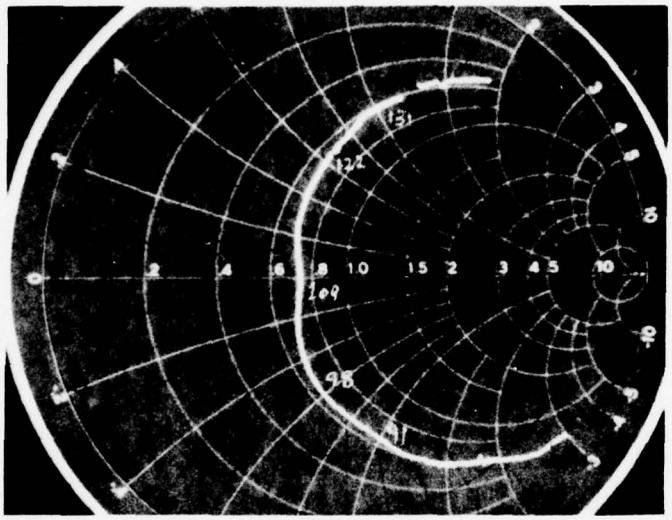

Fig. 13

III. APPENDICES

July - December Publications

A. P. M. Grant and G. S. Kino, "Adaptive Filter Based on SAW Monolithic Storage Correlator," Electr. Lett., vol. 14, no. 17, 17 Aug. 1978, pp. 562-564.

B. J. E. Bowers, B. T. Khuri-Yakub, G. S. Kino, and K-H Yu, "Design and Applications of High Efficiency Wideband SAW Edge Bonded Transducer," presented at 1978 Ultrasonics Symposium, September 1978, Philadelphia, Pennsylvania.

C. H. C. Tuan, P. M. Grant, and G. S. Kino, "Theory and Application of Zinc-Oxide-on-Silicon Monolithic Storage Correlators," presented at 1978 Ultrasonics Symposium, September 1978, Philadelphia, Pennsylvania.

ADAPTIVE FILTER BASED ON S.A.W. MONOLITHIC STORAGE CORRELATOR

Indexing terms: Correlators, Signal processing, Surface-acoustic-wave devices

Design of a wideband adaptive filter incorporating a surface-acoustic-wave monolithic zinc-oxide-on-silicon storage correlator is reported. Its operation is demonstrated with experimental measurements of c.w. interference suppression in a simulated spread-spectrum system. These processors, which are capable of adaptive filtering over 1-20 MHz signal bandwidths in real time, offer significant advantages in terms of complexity and power consumption over equivalent digital systems.

Introduction: Adaptive tapped transversal filters[1] which operate by iteratively adjusting the tap weights with a feedback control loop to achieve some desired filter response, have many diverse applications. They can be used in narrowband (kHz) systems for monitoring low-level foetal heartbeat[1] or for equalisation of the distortion in a telephone channel.[2] At wide (MHz) bandwidths adaptive filtering is used for inverse filtering to improve the range resolution of a radar[3] system or to suppress c.w. interference[4] in a spread-spectrum system.

This letter describes a new realisation of an adaptive filter based on an analogue wideband (1-20 MHz) surface-acoustic wave (s.a.w.) programmable monolithic storage or memory correlator.[5] It operates by storing directly a sample of the input signal, to implement a narrowband filter, which is subsequently used to null out the interference. A prototype adaptive filter is demonstrated suppressing narrowband interference in a simulated spread-spectrum receiver.

Adaptive filter application in interference suppression: Spread-spectrum receivers often experience very high levels of interference, which prevent demodulation of the received message even after matched-filter processing. Wideband interference is suppressed by spatial processing in an adaptive array[1,4,6] while narrowband interference is suppressed in an adaptive transversal filter. One possible implementation of this latter processor is shown in Fig. 1.

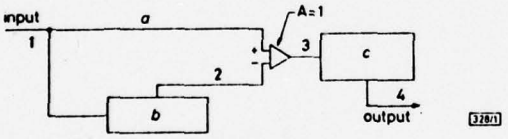

Fig. 1 *Adaptive spread-spectrum receiver*
- *a* Wideband signal with high-level c.w. interference
- *b* Adaptive narrowband filter
- *c* Fixed coded transversal filter

Here a programmable notch filter is realised by loading and storing a sample of the input signal in an s.a.w. correlator.[5] As the narrowband c.w. interference is considerably larger than the wideband coded signal, the correlator impulse response comprises a burst of c.w. whose duration equals the delay across the semiconductor interaction region. Thus it implements a filter with a narrowband $\sin x/x$ frequency response which is automatically set on the interfering frequency. When incorporated as in Fig. 1, the s.a.w. device filters out only the interfering signal at 2, which is subsequently amplified to overcome the loss in the filter and added in antiphase with the input signal. This implements a wideband filter with a notch centred on the interference frequency. Provided that the notch is narrow with respect to the wideband coded signal then there is minimal distortion in the wideband signal.[7] After interference cancellation, the coded signal can then be detected in the receiver matched filter.

Interference cancellation with s.a.w. storage correlator: Wideband s.a.w. devices offer the capability of implementing these adaptive processors at 1-20 MHz signal bandwidths. We are particularly interested in using the zinc-oxide-on-silicon storage correlator[5] which we are developing in our laboratory. This device comprises a silicon wafer with diffused *pn* diodes which is overlaid by a 1·6 μm thick sputtered zinc-oxide film which supports the s.a.w. propagation. It currently offers programmable transversal filtering for waveforms of 4 μs duration and 8 MHz bandwidth.

The test scheme adopted for the practical verification of the adaptive filter is shown in Fig. 2. Here the switches are set in position 1 for signal storage while the adaptive filter operation is performed in position 2, where the bold lines show the signal path. We elected to utilise a short (< 1 μs) gated burst of c.w. in place of a high-voltage impulse to energise the storage diodes. This assures complete saturation of the diodes, and removes the adaptive filter sensitivity to input signal amplitude.

For an input sinusoid $\cos \omega t$ inserted at port A which interacts with a short storage pulse of the same frequency at port B, after a delay T_0 through the inactive region in the device, the stored signal is given by the relation

$$K \int \cos \omega(t - x/v - T_0) \cos \omega t \, dt \qquad (1)$$

$$\approx K \cos \omega(x/v - T_0) \qquad (2)$$

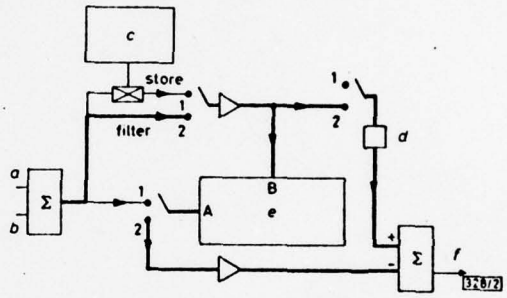

Fig. 2 *S.A.W. implementation of narrowband interference canceller*
- *a* High-level c.w. interference
- *b* Wideband *pn* p.s.k. coded signal
- *c* Store pulse generator
- *d* Attenuator
- *e* S.A.W. storage correlator
- *f* Cancelled output

where K is a constant, x is the spatial distance of the stored signal from the input transducer, and v is the propagation velocity. Thus the spatial stored charge pattern corresponds exactly to the input signal. If now, after storage, a later time sample of signal, $\cos \omega t$ is inserted into the device at port B, the output at A, after passing through the same delay T_0, is

$$F(t) = \alpha \int_0^L \cos \omega(x/v - T_0) \cos \omega(t - x/v - T_0) \, dx \qquad (3)$$

$$\approx (\alpha/2) \cos \omega t \qquad (4)$$

where α is a constant of the device and L is the length of the semiconductor interaction region. Thus the time delay T_0 cancels out and the delayed filter output is always in phase with the input. Provided that the store pulse saturates the diodes then the filter will have a constant insertion loss, independent of the input power level. Once the processor is adjusted at a particular frequency, ω, the parameter α can be determined and exact phase cancellation will be obtained for any input c.w. frequency within the bandwidth of the device.

Fig. 3*a* shows the signal input to our s.a.w.-based adaptive processor. It comprises a +10 dBm, 121·8 MHz c.w. signal plus a −10 dBm, 6·2 μs burst of 31-chip *pn* code, modulated at 5 MHz rate onto 120 MHz carrier. The direct correlation of this composite signal in the 31-chip matched filter, without the adaptive processor, is shown in Fig. 3*b*. For adaptive

Reprinted from ELECTRONICS LETTERS 17th August 1978 Vol.14, No.17 pp. 562–564

filter operation a 4 μs sample of the c.w. signal was stored in the correlator by pulsing the top plate with an amplifier +20 dBm 200 ns burst of the input 121·8 MHz waveform, Fig. 2. Cancellation was achieved by summing the +40 dB amplified filter output with the 30 dB attenuated input, ensuring that the signal phases are arranged as in Fig. 2. This implements a flat-amplitude-characteristic filter with a single notch at the interference frequency. Our correlator, which stored a $T = 4\,\mu s$ input sample, where $T = L/v$ is the time delay of an acoustic wave passing through the semiconductor

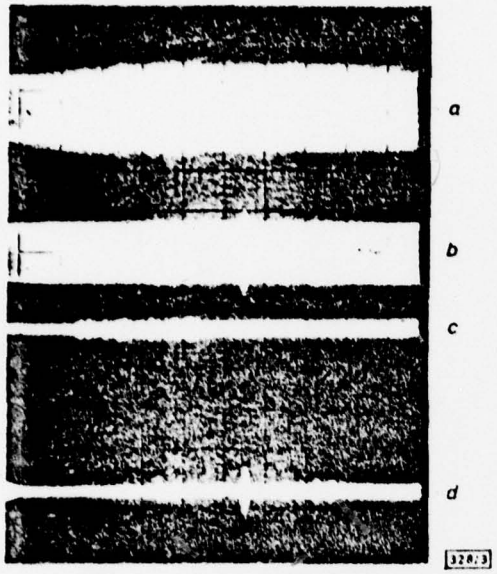

Fig. 3 *S.A.W. adaptive-filter demonstration*

Horizontal scale: 2 μs per large division

- *a* Input waveform prior to adaptive processing. It comprises a 121·8 MHz c.w. plus a 5 MHz clock rate 31-chip *pn*-p.s.k. coded sequence, centered on 120 MHz at −20 dB relative power level
- *b* Direct correlation of (*a*) in 31-tap s.a.w. fixed coded matched filter
- *c* Waveform after adaptive processing in s.a.w. storage correlator which cancelled out high-level narrowband interference by 20 dB
- *d* Correlation of (*c*) in 31-tap s.a.w. fixed coded matched filter

region, realised a 20 dB deep notch whose width was approximately 250 kHz ($1/T$). A comparison between the input signal trace (Fig. 2*a*) and the cancelled output signal trace (Fig. 2*c*), clearly shows the 20 dB suppression of the 121·8 MHz interference, leaving the wideband coded signal clearly visible. The adaptive interference canceller permitted the correlation peak from the final matched filter (Fig. 1) to be clearly detected (Fig. 2*d*). We have also shown that after our processor is set up and optimised it can simultaneously notch out one or more interfering frequencies anywhere within the 8 MHz bandwidth of our s.a.w. storage correlator. This capability is achieved as the cancelling signal from the filter and the input signal are always in antiphase with our storage arrangement.

Conclusion: We have demonstrated the potential application of the s.a.w. storage correlator for the suppression of single or multiple interfering signals. The processor adapts automatically after storing a sample of the interfering signal. With improved amplitude and phase matching we believe that our processor can achieve 30–40 dB notch suppression. Further improvements can be obtained with adaptive feedback control[1,4] of the tap weights. Thus we suggest that this demonstration is a first step to the more general adaptive equaliser. Therefore we believe that current s.a.w. storage correlators,[5,8] which are equivalent to transversal equalisers processing 1–20 MHz signal bandwidths with 16–200 complex tap weights, have considerable future potential for adaptive signal processing in radar communication and imaging systems.

Acknowledgments: The assistance of H. C. Tuan in designing and constructing the storage correlator and helpful discussions with B. Widrow and W. K. Masenten are gratefully acknowledged. This work was supported by the Defense Advanced Research Projects Agency through the Office of Naval Research under Contract N00014-76-C-0129.

P. M. GRANT
G. S. KINO

Edward L. Ginzton Laboratory
Stanford University
Stanford
California 94305
USA

18th July 1978

References

1 McCOOL, J. M., and WIDROW, B.: 'Principles and applications of adaptive filters', *in* IEE Conf. Publ. 144, 1976, pp. 84–95
2 LUCKY, R. W.: 'Automatic equalization for digital communications', *Bell Syst. Tech. J.*, 1965, 44, pp. 547–588
3 MAINES, J. D., *et al.*: 'Inverse filter: design and performance using surface acoustic waves', IEEE Ultrasonics Symposium Proceedings, 1973, pp. 437–440
4 WIDROW, B., *et al.*: 'Adaptive noise cancellation: principles and applications', *Proc. IEEE*, 1975, 63, pp. 1692–1716
5 TUAN, H. C., KHURI-YAKUB, B. T., and KINO, G. S.: 'A new zinc-oxide-on-silicon monolithic storage correlator', IEEE Ultrasonics Symposium Proceedings, 1977, pp. 496–499
6 COMPTON, R. T.: 'An adaptive array in a spread spectrum communication system', *Proc. IEEE*, 1978, 66, pp. 289–298
7 SUSSMAN, S. M., and FERRARI, E. J.: 'The effects of notch filters on the correlation properties of a PN Signal', *IEEE Trans.* 1974, AES-10, pp. 385–390
8 RALSTON, R. W., *et al.*: 'Improved acoustoelectric Schottky-diode/$LiNbO_3$ memory correlator', IEEE Ultrasonics Symposium Proceedings, 1977, pp. 472–477

0013-5194/78/170562-03$1.50/0

Appendix B

DESIGN AND APPLICATIONS OF HIGH EFFICIENCY WIDEBAND SAW EDGE BONDED TRANSDUCERS

BY

J. E. Bowers, B.T. Khuri-Yakub, G. S. Kino, and K-H Yu

Preprint

G.L. Report No. 2867

September 1978

Contracts

N00014-76-C-0129

and

NSF Grant ENG77-28528

to appear in
1978 Ultrasonics Symposium Proceedings

Edward L. Ginzton Laboratory
W. W. Hansen Laboratories of Physics
Stanford University
Stanford, California

DESIGN AND APPLICATIONS OF HIGH EFFICIENCY WIDEBAND SAW EDGE BONDED TRANSDUCERS

J. E. Bowers, B. T. Khuri-Yakub, G. S. Kino, and K-H Yu
Edward L. Ginzton Laboratory
Stanford University
Stanford, California 94305

Abstract

Edge bonded transducers (EBTs) have the potential to be efficient and broadband SAW transducers for signal processing and nondestructive testing applications. A normal mode theory has been developed for the design of EBTs. EBTs have been made for SAW propagation on Quartz and Silicon Nitride ceramic, and the early results are in good agreement with theory.

Introduction

There has been a great deal of interest in exciting Surface Acoustic Waves (SAW) on nonpiezoelectric media for both signal processing and nondestructive testing applications.[1,2] For this purpose, typically, piezoelectric films such as Zinc Oxide (ZnO) are deposited on the nonpiezoelectric substrates, and Interdigital Transducers (IDT) are used. The main problem with such transducers is their low efficiency and small bandwidth. Lardat et al[3,4] showed experimentally that Edge Bonded Transducers (EBT) can be employed to yield a higher efficiency and larger bandwidth than an IDT, and have the additional advantage that they can be used with a nonpiezoelectric substrate. In this work we have developed a quantitative theory to predict the design parameters of EBTs. We have also built EBTs and the early results tend to confirm our theory experimentally.

A schematic diagram of an edge bonded transducer is shown in Fig. 1. The depth and width of the back contact controls the impedance and efficiency of the EBT, while the thickness of the piezoelectric layer determines its center frequency. The ceramic piezoelectric layer is poled in a direction normal to the surface of the substrate and to the direction of propagation of the surface wave, so as to provide mainly shear wave excitation.

Consider the excitation of an acoustic wave by a charge distribution corresponding to the charge on the electrodes:

$$\rho(x,y,z) = [\delta(x+\ell/2) - \delta(x-\ell/2)]\sigma(y,z) \quad (1)$$

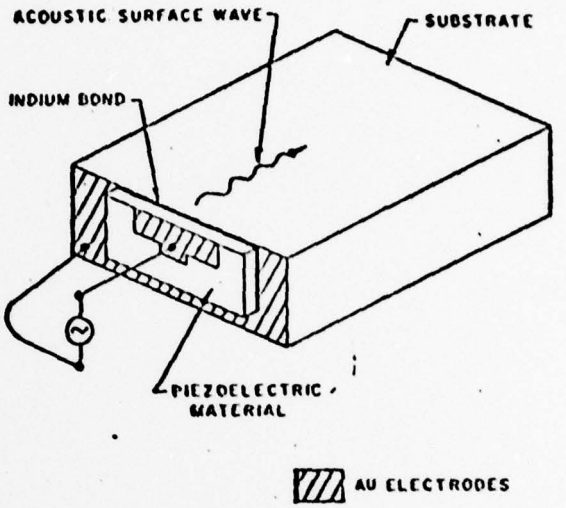

AN EDGE BONDED TRANSDUCER

FIGURE 1

as shown schematically in Fig. 2. Following Auld and Kino,[5] we can expand the electric potential associated with the acoustic waves in normal modes of the form:

$$\phi(x,y,z) = \sum_n a_n(x)\,\phi_n(y,z) \quad (2)$$

where a_n is the amplitude of the n^{th} mode, $a_n a_n^* P_n$ is the power in the n^{th} mode and ϕ_n the voltage of the n^{th} mode for a power P_n. Following the treatment of reference 5 we can write

$$\frac{\partial a_n}{\partial x} + j\beta_n a_n = \frac{j\omega}{4P_n}\int \rho(x,y,z)\phi_n^*(y,z)\,dydz \quad (3)$$

1978 Ultrasonics Symposium Proceedings
IEEE Cat. #78CH 1344-1SU

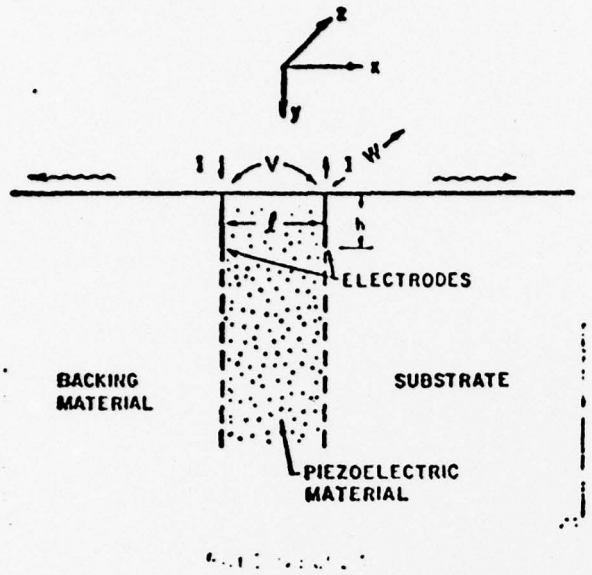

FIGURE 2. Planar cross section of a backed edge bonded transducer.

A variational expression for the electrical input impedance of the transducer,[5] can be written in the form

$$Z = \frac{\int \Phi(x,y,z)\ \rho(x,y,z)\ dxdydz}{j\omega Q^2} \qquad (4)$$

The input voltage V at the terminals can be defined in terms of Z and the input current $I = j\omega Q$, as

$$V = ZI = j\omega QZ \qquad (5)$$

The potential has two contributions $V = V_a + V_c$ where V_a is the potential due to the acoustic wave, and V_c the electrostatic potential due to the charge $Q = \int \sigma(y,z)dydz$. So it follows that

$$V_c = I/j\omega C_0 \qquad (6)$$

where C_0 is the geometric capacitance of the transducer.

We keep only the terms in Eq. (2) corresponding to the backward and forward propagating surface wave modes denoted by a subscript 1, although the expression can be solved more generally.

Because we are dealing with a mode whose voltage distribution is nonuniform over the cross section of the transducer, it is necessary to define the dimensionless parameter α_1 for the potential of the acoustic surface wave modes, by writing

$$\alpha_1 = \frac{1}{h}\int_0^h \phi_1(y)/\phi_1(o)\ dy \qquad (7)$$

where it has been assumed that ϕ_1 is uniform with z and the charge density $\sigma(y,z) = Q/A$.

We also define an electrical impedance of the mode in a standard way as

$$Z_1 = \frac{\phi_1(o)\ \phi_1^*(o)}{2P_1} \qquad (8)$$

After solving Eq. (3) and inserting it in Eq. (4) with the use of Eqs. (1) and (2), we find after considerable algebra that we can express the results in terms of the Krimholtz, Leedom, and Matthaei[6] equivalent circuit for a bulk wave transducer, as shown in Fig. 3, where now the impedance of the transmission line is defined as Z_1, and the transformer ratio as

$$\phi = 2\alpha_1 \sin \beta_1 l/2 \qquad (9)$$

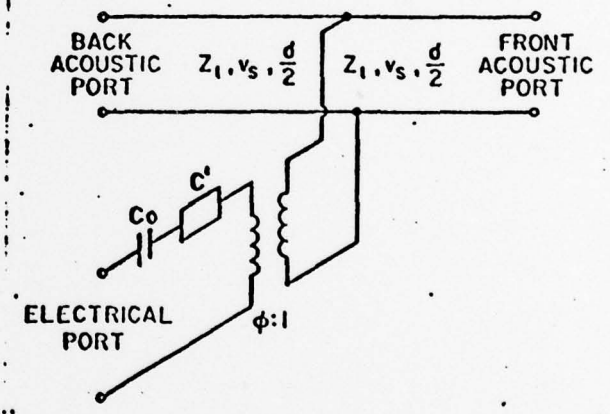

FIGURE 3. Transmission line model of piezoelectric EBT (after Krimholtz, Leedom, and Matthaei).

with the series reactance in the circuit defined as

$$Z_e = j\alpha_1^2 Z_1 \sin \beta_1 \ell \qquad (10)$$

At the half wave resonance ($\omega = \omega_0$, $\beta_1 \ell = \pi$), it follows that the input impedance of the circuit is $R_{a0} + 1/j\omega C_0$, where

$$R_{a0} = 4\alpha_1^2 Z_1 / S \qquad (11)$$

with

$$S = \frac{1+\Gamma_L}{1-\Gamma_L} + \frac{1+\Gamma_R}{1+\Gamma_R} \qquad (12)$$

and Γ_L, Γ_R are, respectively, the reflection coefficients of the surface wave on the left hand and right hand side of the transducer. For a matched air backed transducer $S = 1$.

It has been shown that for an acoustic surface wave[6]

$$Z_1 = \frac{2\Delta v/v}{\omega c w} \qquad (13)$$

where $\Delta v/v$ for a surface wave is defined in the normal way and

$$c = \left(c_{11}^T c_{33}^T - c_{13}^{T2}\right)^{1/2} .$$

So as $C_0 = \epsilon_{11}^S wh/\ell$, we can calculate the effective electrical Q of the tuned transducer, $Q_e = 1/\omega_0 C_0 R_{a0}$ as well as its efficiency, by using the quantity $\omega_0 C_0 R_{a0}$ as a criterion of quality. We write

$$\left(\omega_0 C_0 R_{a0}\right)_{EBT} = \frac{8}{\pi} \alpha_1^2 \beta_1 h \frac{\Delta v}{v} \frac{\epsilon_{11}}{cS} \qquad (14)$$

For an interdigital transducer of N finger pairs, it can be shown that with the spacing equal to the finger width

$$\left(\omega_0 C_0 R_{a0}\right)_{ASW} = 2.87 N \Delta v/v \qquad (15)$$

While for a bulk wave shear wave transducer, it can be shown that

$$\left(\omega_0 C_0 R_{a0}\right)_{bulk} = 4\bar{k}^2/\pi S \qquad (16)$$

where $\bar{k}^2 = k_{15}^2/(1+k_{15}^2)$.

We now make a rough comparison of the optimized EBT with the other two transducers. We have calculated $(\Delta v/v)/k_{15}^2$ for GaAs, ZnO, quartz, and $LiNbO_3$ and PZT-5A. The value of this parameter varies from 0.047 to 0.053; we take 0.05 as a reasonable average.

Similarly the potential of a surface wave for most surface wave materials falls off approximately as $\exp -y/\lambda$. It then follows that with this assumption

$$\left(\omega_0 C_0 R_{a0}\right)_{EBT} = 16 \frac{\epsilon_{11}}{cS} \frac{\left(1-e^{-h/\lambda}\right)^2}{h/\lambda} \frac{\Delta v}{v} \qquad (17)$$

Thus for $(\omega_0 C_0 R_{a0})$ to be maximum $h/\lambda \approx 1.3$ with a very flat maximum and with $S = 1, \epsilon_{11}^S \approx c$

$$\mathrm{Max}\left(\omega_0 C_0 R_{a0}\right)_{EBT} \approx 6.5\, \Delta v/v \qquad (18)$$

It follows that, as might be expected, the EBT would have over twice the electronic bandwidth of the ideal one finger pair transducer. This is because of the higher value of R_{a0} obtained with the air backing due to the addition of the forward and backward waves. Here, however, the capacity of the transducer is also over twice that of the single pair transducer, and a much higher dielectric constant material such as a piezoelectric ceramic can be employed to keep the impedance to a value suitable for matching to a 50-ohm circuit, with a transducer of reasonable width w.

Taking $[(\Delta v/v)/k_{15}^2] = 0.05$, we see that

$$\frac{\left(\omega_0 C_0 R_{a0}\right)_{EBT}}{\left(\omega_0 C_0 R_{a0}\right)_{bulk}} \approx 0.25\, k_{15}^2/\bar{k}^2 .$$

For PSN with $k_{15}^2 \approx 0.35$ this gives a ratio of 0.330. Thus the optimum matched EBT would have an electronic bandwidth of the order of one-third of that of a bulk wave transducer of the same material. But by choosing a lower impedance medium for surface wave propagation than that of the transducer material, the bandwidth can be optimized to approximately 60% of the equivalent bulk wave transducer. Because the acoustic bandwidth of an EBT transducer is of the order of 100%, very large bandwidths can be obtained, with lower efficiencies. A further contribution to large acoustic bandwidth is the fact that for $\lambda/h < 1$, R_{a0} will tend to be fairly uniform with frequency, while for a bulk wave transducer $R_{a0} \propto 1/\omega$. So at the expense of a loss in efficiency, it is possible to design extremely wide bandwidth EBTs.

Experimental Design and Results

Following the work of Lardat, we decided to employ PSN (potassium sodium niobate) as the transducer material. The high dielectric constant is a vital requirement to obtain an input impedance of the order of 50 ohms with a reasonable width transducer. Furthermore, PSN is the only ceramic of which we are aware, which can be operated in the 100 MHz range. Some of the material constants

for PSN were taken from Jaffé and Berlincourt[8] and some have been measured by us in separate experiments. Our estimates of its material constants are given in Table I. We used these parameters to carry out a calculation for a_1 and $\Delta v/v$ of PSN using a program due to Wagers.[3] We had difficulty doing this because the ASW appears to have a leaky wave when there is no short circuit at the surface. But we were able to estimate $\Delta v/v$ to be 1.7×10^{-2}. Figures 5 and 6 show the theoretical input impedance and the two-way untuned insertion loss from a 50-ohm source as a function of frequency and width of the transducer of an EBT on silicon nitride (Si_3N_4) where we have chosen the reflection coefficients by using shear wave impedance parameters. The transducer has a thickness $\ell = 35$ μm which corresponds to a resonant frequency of 44.3 MHz. The depth of the back plate is $h = 60$ μm corresponding to $h/\lambda = 0.86$. The optimum choice would have had $h/\lambda = 1.3$ somewhat larger than this value.

Table I

PSN properties estimated from our measurements and Berlincourt and Jaffé

$$c_{11}^E = 20.9 \times 10^{10} \ N/m^2$$
$$c_{12} = 11.6 \times 10^{10}$$
$$c_{13} = 11.7 \times 10^{10}$$
$$c_{33} = 18.3 \times 10^{10}$$
$$c_{44} = 3.8 \times 10^{10}$$
$$c_{66} = 4.65 \times 10^{10}$$
$$e_{11}^S = 435\, \epsilon_0$$
$$e_{33}^S = 306\, \epsilon_0$$
$$e_{z1} = -1.72 \ m^2/c$$
$$e_{z3} = 7.86$$
$$e_{x5} = 11.3$$
$$k_{15} = 0.59$$
$$\Delta v/v = 0.17$$
$$\rho = 4.51 \times 10^3 \ kg/m^3$$

At 40 MHz with $\ell = 35$ μm, $h = 60$ μm, $1/\omega_0 C_0 = 50$ ohms, the optimum value of C_0 for an untuned transducer, when

$$w = \ell/50\omega_0 c_{11}^S h \quad \text{or} \quad w' = 12 \text{ mm}.$$

Because a_1 and z_1 vary with frequency the frequency dependence of the transducer response is different from that of a bulk wave transducer when the bandwidth is large. As can be seen from Figs. 4 and 5, the 3 dB bandwidth with approximately 14 dB return loss should be of the order of 70%. Under the same conditions with a 50-ohm source a series tuned 2 mm wide transducer would have somewhat less bandwidth, of the order of 50%. We note that $K_{33}\omega_0 C_0$ for this transducer is 0.10, a result in agreement with that obtained by our rough estimate of Eq. (16).

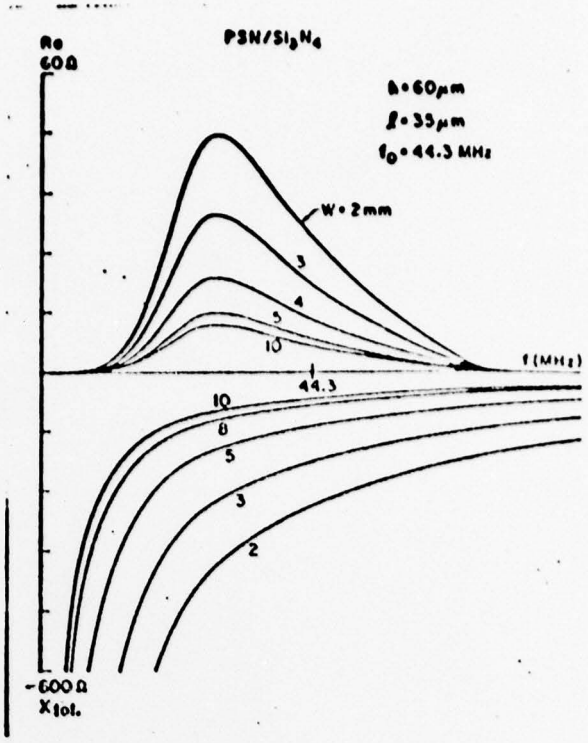

FIGURE 4. Theoretical input impedance of EBT vs frequency for different values of beam width.

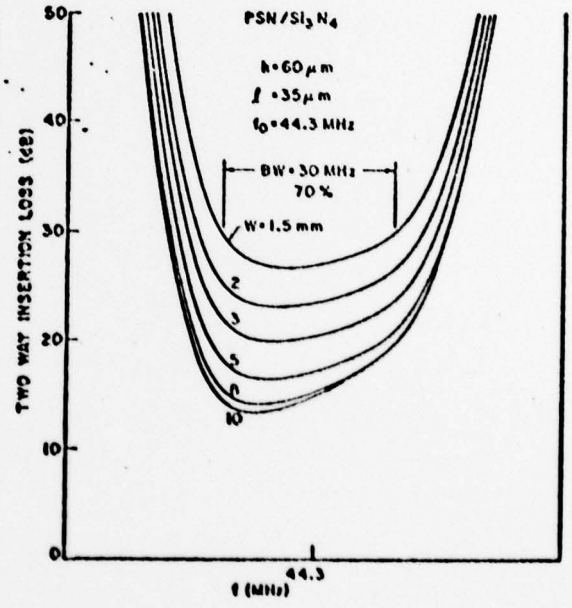

FIGURE 5. Theoretical untuned two-way insertion loss of EBT vs frequency for different values of beam width.

Because of our interest in Nondestructive Evaluation, we have built an edge bonded transducer on Si_3N_4. The beam width we used was 2.0 mm, for which the theoretical untuned insertion loss is 23 dB. We measured the insertion loss by measuring the amplitude of the reflection from a 90° corner. The reflection coefficient of a 90° corner in a material with a Poisson's ratio of $\sigma = 0.25$, is equal to -12 dB.[10] We measured a total terminal-to-terminal insertion loss of -43 dB which compares favorably with a theoretical prediction of -35 dB. The fractional bandwidth was measured to be 25%, which is much smaller than the theoretically predicted value of 70%. The impulse response of the transducer is compared to theory in Fig. 6 which shows a reasonable agreement. Contact was made to the transducer by bonding a 1 mil gold wire across the width of the back plate. This contact resulted in the trailing echo in the impulse response of Fig. 6 and hence the decreased bandwidth of the transducer. We are presently making better masks to overcome this problem and construct more efficient and broadband EBTs.

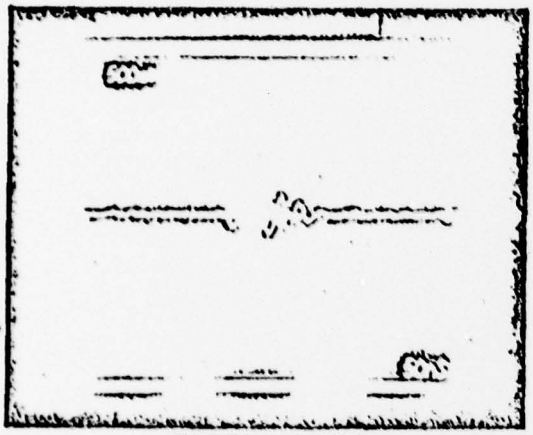

FIGURE 6. Comparison of theoretical and experimental impulse responses.

A normal mode theory has been developed to design EBTs. Our theory is in good agreement with our preliminary results and those of other workers in the field.

Acknowledgement

This work was supported partly by the Defense Advanced Research Projects Agency and monitored by the Office of Naval Research under Contract No. N00014-76-C-0129 and partly by the National Science Foundation under Grant No. ENG77-28528.

References

1. H. C. Tuan, B. T. Khuri-Yakub, and G. S. Kino, IEEE Proceedings of the Ultrasonic Symposium (1977), pp. 496-499.

2. B. T. Khuri-Yakub and G. S. Kino, Appl. Phys. Letters 39(9) (1 May 1978), pp. 513-514.

3. C. Lardat and P. Defranould, Proc. IEEE 64, #5 (May 1976), pp. 627-630.

4. C. Lardat, IEEE Proceedings of the Ultrasonic Symposium (1974), pp. 433-436.

5. B. A. Auld and G. S. Kino, IEEE Trans. Electron Devices ED-18, #10 (October 1971), pp. 898-908.

6. R. Krimholtz, D. Leedom, and G. Matthaei, Electronics Letters 6 (June 1970), pp. 398-399.

7. C. DeSilets, J. Fraser, and G. S. Kino, IEEE Trans. on Sonics and Ultrasonics SU-25, #3 (May 1978), pp. 115-125.

8. H. Jaffé and D. A. Berlincourt, Proc. IEEE 53, #10 (October 1965), pp. 1372-1386.

9. R. S. Wagers, Ph.D. Dissertation, Stanford University (1972).

10. F. Cuozzo, E. L. Cambiaggio, J. Damiano, and E. Rivier, IEEE Trans. on Sonics and Ultrasonics SU-24 (1977), pp. 280-289.

Appendix C

THEORY AND APPLICATION OF ZINC-OXIDE-ON-SILICON MONOLITHIC STORAGE CORRELATORS

by

H. C. Tuan, P. M. Grant, and G. S. Kino

Preprint

G.L. Report No. 2872

October 1978

Contract

N00014-76-C-0129

presented at the
1978 Ultrasonics Symposium

Edward L. Ginzton Laboratory
W. W. Hansen Laboratories of Physics
Stanford University
Stanford, California

THEORY AND APPLICATION OF ZINC-OXIDE-ON-SILICON MONOLITHIC STORAGE CORRELATORS

H. C. Tuan, P. M. Grant, and G. S. Kino
Edward L. Ginzton Laboratory
Stanford University
Stanford, California 94305

Abstract

A new theory has been developed for the storage mechanism of the P-N diode which takes into account the minority carrier lifetime. Close agreement is demonstrated with experimental results from a single diode model. The theory is extended to the SAW monolithic storage correlator and is found to fit closely to measured results.

Potential applications for storage correlators are also surveyed. Operation in the input correlation mode, with time bandwidth (TB) products between 10^3 and 10^6, offers application in programmable Fourier transformation, spread spectrum synchronization and adaptive filtering. An adaptive signal processor is described which is capable of suppressing narrowband interference in a spread spectrum system.

1. Introduction

In last year's symposium we described our theoretical and experimental work on airgap[1] and ZnO-on-Si surface wave correlators.[2] We showed that we were able to obtain storage by inserting a signal into one acoustic port and applying a short pulse to the center electrode. At the time, we postulated that with a p-n diode system it is possible to obtain efficient storage with very short pulses, of the order of 1/2 rf cycle long, and carried out a theory based on this hypothesis. Later, it was found that these results did not agree well with those of others, or with our own results on the ZnO-on-Si correlator. The reason for the discrepancy is that the particular MESA diode configuration employed had very short recombination times. Furthermore, as has been suggested by Emtage,[3] the recombination time under forward bias is much shorter than in the backward bias regime because the recombination trap involved is not at the center of the band.

In this paper, we first describe results obtained on the ZnO-on-Si correlator with more conventional p-n diodes in which the recombination time is of the order of 300 nS – 3 μS. The results obtained, when the diodes are excited directly through a capacitor, are in excellent agreement with our theoretical predictions. Furthermore, the variation in the amplitude of the stored output as a function of input amplitude agrees extremely well with the theory, which has been extended from the original airgap theory that we carried out earlier.

Last year, we described the use of the ZnO-on-Si storage correlator in an input correlation mode.[1,2] In this mode, two signals are simultaneously applied to an acoustic port, and the center electrode respectively. The individual diode stores a component of signal which is proportional to the integral of the product of these input signals as a function of time. So, in fact, the correlation of the input signals is read into and stored in the correlator diode array. As the input signals can be read in over a period much longer than the time delay through the device, i.e., to the storage time in the device, it is possible to correlate signals with very large time bandwidth products. However, at that time, we and others believed that this mode was basically highly nonlinear and that correlation could only be obtained over a very limited dynamic range.

Recently we have carried out a series of experiments which demonstrate that in fact this device can be operated linearly in the input correlation mode. The output signal obtained by interrogating the device with a short readout pulse, is linearly proportional to the amplitudes of each one of the input signals and to the correlation time employed. These results have been carried out with correlation times in the range 30 μsec to 100 msec. However, the most linear results are obtained with correlation times of less than 10 msec. We have performed these measurements both with single frequency rf pulses and by correlating PSK codes up to 10 msec. Similar results have also been obtained with chirp signals, where we were implementing a variable resolution Fourier transform, but they will not be described in this paper. Finally, by applying these techniques, we have been able to construct an adaptive filter to remove a high level interfering CW signal from a PSK code. Here we carry out input correlation of the input signal, and form a narrowband filter which responds only to the CW signal. This narrowband filter can then be used in a bridge circuit to eliminate the interfering CW signal.

1978 Ultrasonics Symposium Proceedings
IEEE Cat. #78CH 1344-1SU

Tuan, Grant, Kino

II. Theory of the ZnO-on-Si Monolithic Storage Correlator

The basic storage element of the monolithic storage correlator is a p-n diode in series with a capacitor. Since the p-n diode is a minority carrier device, it normally cannot respond rapidly enough to store 100% of the injected charge from a short pulse. In our ZnO correlator the correlation efficiency obtained with this so-called "flash" mode of operation is always 15-20 dB lower than that obtained with the rf writing mode. We have developed the theory of the transient charging of the p-n diode which takes account of recombination of minority carriers injected into the neutral region.

When the positive pulse is applied to a capacitor-diode circuit it turns on the diode and minority carriers (holes) are injected from the p-side of the junction to the n-side, and diffuse into neutral region. Since the store pulse is usually short (5 - 10 nsec), the diode can stay forward biased only for a few nanoseconds, and after that it becomes reverse biased. Most of the minority carriers then return to the p layer and the associated current discharges the series capacitor. Consequently, these carriers do not contribute to the long-term storage effect of the device. The only carriers that can contribute to the long-term storage effect are the ones which have been recombined during this short period.

Thus if $Q_p(t)$ is the total minority carriers charge stored in the neutral region, then the amount of charge Q_c which remains in the capacitors after the charging process is over is simply

$$Q_c = \int_0^\infty \frac{Q_p(t)}{\tau_p}\, dt \qquad (1)$$

where τ_p is the recombination time.

We have worked out both analytic and numeric solutions to calculate the function $Q_p(t)$. The total charge stored is found to be inversely proportional to the square root of the minority carrier lifetime. We have also checked the theory by measuring the response of a circuit which consists of a 1 mm^2 p-n diode in series with externally connected capacitor and resistor. The agreement between the theoretical predictions and the experimental results is excellent.

To calculate the correlation efficiency of the device, a normal mode analysis similar to the one described by Borden and Kino[1] has been developed for the monolithic storage correlator. When this theory is combined with the new charging theory for the p-n diode, it predicts very well the performance of the device, Fig. 1, where the correlation output is plotted against the amplitude of the narrow pulse used. The choice of 300 - 400 nsec as the minority carrier lifetime has been justified by measurement in the RF writing mode where the correlation output starts to saturate after the duration of the RF writing signal exceeds about 400 nsec.

The shift between the theoretical curve and the experimental curve at low pulse amplitude is partially due to the parasitic capacitance between the plate electrode and the n-regions between diodes and partially due to the fact that the actual depletion capacitance of the diode is larger than that calculated from the area of the p^+-region.

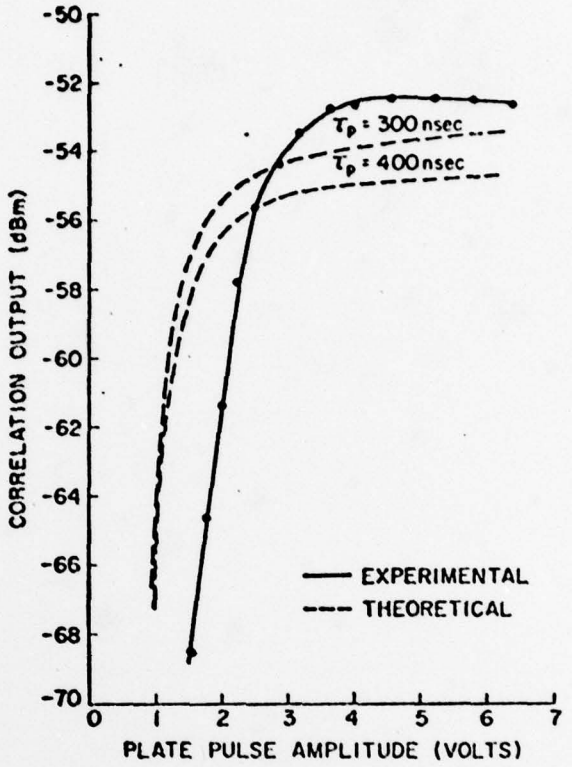

FIGURE 1--Theoretical and experimental stored output of correlator with 5 nS input plate pulse and read out signal of 2V p-p. P_a = 10 dBm.

III. The Input Correlation Mode

We have initially carried out tests on the device performance in this mode using CW signals. When using CW waveforms, instead of coded waveforms, the stored charge pattern occupies the whole length of the diode array and the largest possible output dynamic range is obtained. Thus, we can examine the device operation more accurately. In the past, it was always thought that this input correlation mode was useful only when the signal levels are carefully controlled. The underlying reasoning behind this proposition is confirmed by our measurement, as shown in Fig. 2. Here the plate signal and the acoustic signal are varied at the same time so that their durations are always equal. The correlation output measured in this manner is a good indication of how fast the charging process is. As can be seen, when the plate signal is 1 V p-p, the correlation output is close to being linear with the integration time. But as the amplitude of the plate signal is increased, the correlation output becomes highly

nonlinear with respect to the integration time. In other words, the time required to saturate the storage effect drops drastically with increasing plate signal levels. These high amplitude measurements also confirm the measured results[4] with airgap correlators where the read out correlation amplitude did not significantly alter between 1 mS and 10 mS input correlation period.

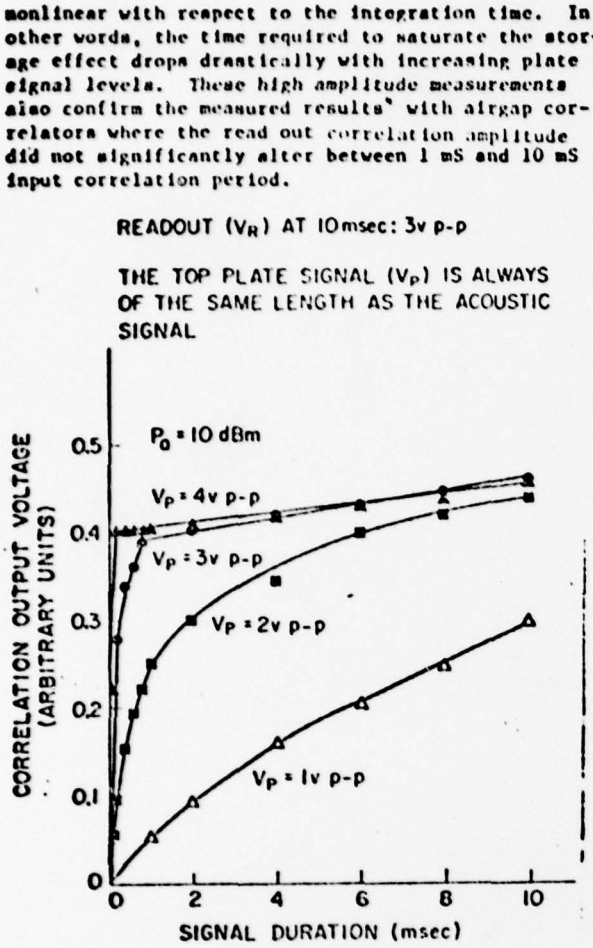

FIGURE 2. Charging characteristics of the diodes with acoustic and top plate signals of same time duration.

We have recently found an alternative highly linear mode of operation, which was suggested by Ralston.[5] Here the length of the reference plate signal is kept constant while the duration of the input signal is varied. This corresponds much more closely to the requirements of signal processing systems. The results of such measurements are shown in Fig. 3. Linear responses as a function of time and the acoustic input voltage are obtained for all the plate signal levels used. It is noted that the output as a function of the integration time is essentially constant for all plate signals larger than 2V p-p. This 2V p-p can thus be considered as a threshold signal level beyond which the output is insensitive to the plate voltage. For shorter integration periods, a larger threshold signals level is required, but still it is much less sensitive to V_p than it was thought to be.

It should be noted, in addition, that the saturation value of the plate voltage is essentially dictated by the value of the reading voltage V_R.

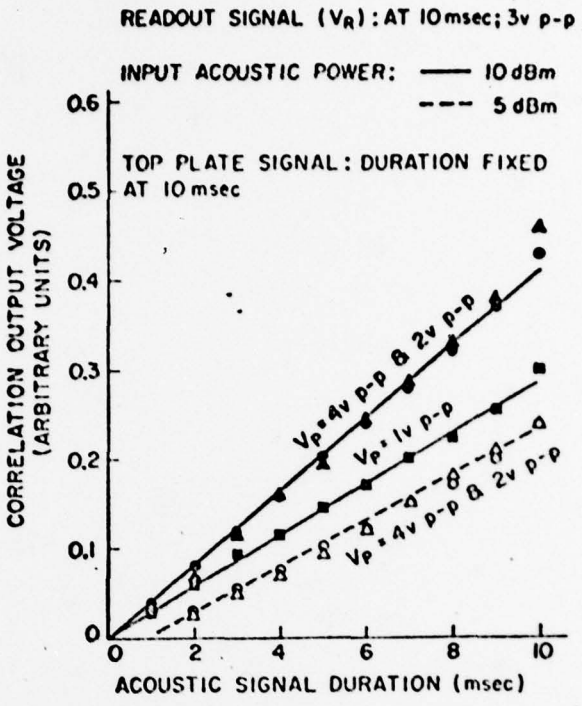

FIGURE 3. Linear integration with the storage correlator when top plate signal fixed at 10 mS duration.

Typically saturation begins to occur when $V_R - V_p < 1V$. We note that again this implies a very different mode of operation from that normally employed, where it is usually assumed that $V_R \ll V_p$. In either case the output is also proportional to V_R. It would seem reasonable to assume, then, that when $V_R \gg V_p$, the action of the reading signal is to switch on the diodes, rather than operating them as back biased varactors as in the theory of Borden and Kino.[1] In this case, the switching point is determined by $V_a + V_p$, so all the output is obtained across the capacity of the piezoelectric layer rather than divided between the ZnO and the diode capacity. This mode of operation, then, in addition to being a highly linear one also provides optimum efficiency and as it uses large signals provides the largest output possible.

It should be pointed out that the voltage levels measured in Figs. 1 - 3 are terminal values. Due to inductance of the lead connecting the terminal to the plate electrode, the actual voltage on the electrode should be reduced by a factor of 2.7 for our structure. The voltage appearing across the diode is further reduced by the presence of series resistance due to the Si substrate.

These results indicate that our storage correlator is highly suitable for synchronization in spread spectrum system, which requires a large time bandwidth product coded correlator.[6] Most previous attempts to realize this with SAW devices

have used either a cascade of matched filters[7] or a single programmable matched filter followed by a recirculating delay line integrator.[8] We show here that the storage correlator can be used directly in the input correlation mode for correlating the large time bandwidth product Pseudo Noise (PN) Phase Shift Keyed (PSK) or PN frequency hopped waveforms used in spread spectrum systems. We have performed detailed measurements on the correlator operation in input correlation mode when processing 5 MHz bandwidth PN-PSK signals to study its linearity with coded signals.

The PN-PSK test signal input was amplified to the maximum power level for operating our transducers (+16 dBm) and fed into the correlator acoustic port. The local reference signal, a delayed PN-PSK code, was amplified to +28 dBm and inserted on the top plate. This wrote the correlation peak into the diode array as a stored charge pattern, which was subsequently read out with a 200 nS high power (+32 dBm) rf readout pulse. Figure 4 shows the read out correlation peaks for three different delays between signal and reference ports, when integrating for 1 mS (TB = 5,000). The power of the output correlation peak after readout was measured as -54 dBm, about 40 dB above the noise level.

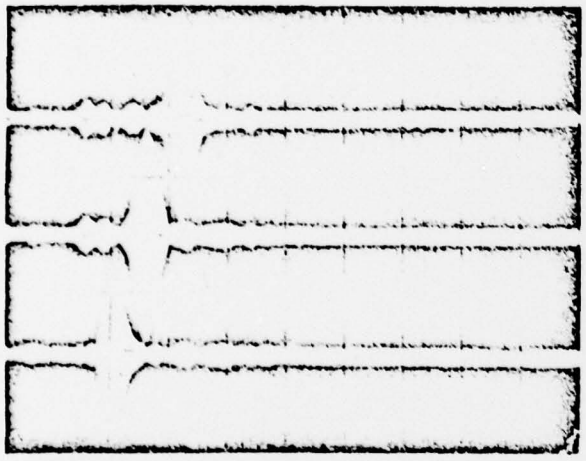

FIGURE 4. Large time bandwidth product PN-PSK matched filter. Scale 1 μS per division.

In order to ascertain the optimum device operating power level and verify linear operation each of the 3 input powers were independently reduced and the correlation peak power measured, Fig. 5. It clearly shows linearity in all three input ports, except at the high levels of drive power on the top plate when the diodes are saturated. The correlator has an "effective" insertion loss of 70 dB which is due predominantly to filling factor loss.[4] With the input powers we selected, we have thus shown that we are operating the device at close to its optimum values.

We have also investigated whether in the input correlation mode the correlation peak amplitude

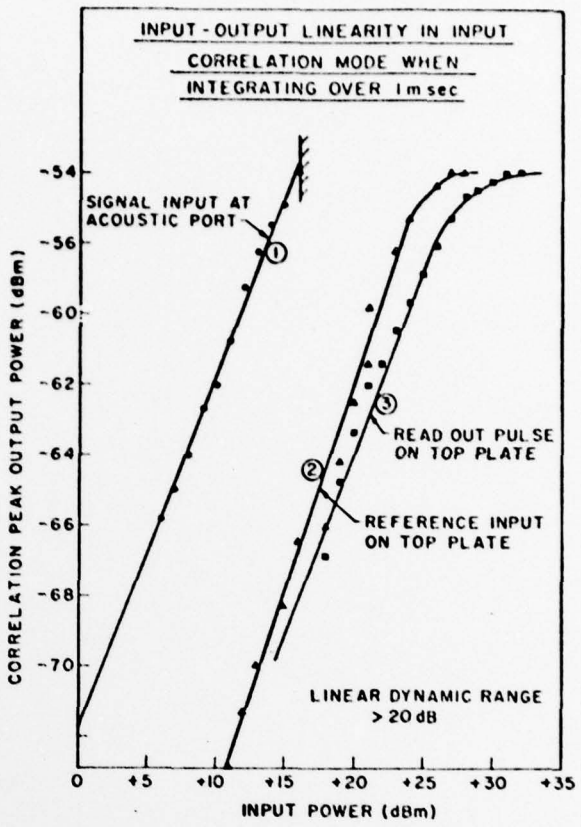

FIGURE 5. Storage correlator linearity measurements.

varies linearly with integration time when processing coded waveforms. This was done by selecting a given maximum integration time (e.g., 1 mS) and setting the reference PN-PSK code to this duration. The duration of the signal sample was again varied from 0 to 1 mS, while maintaining the same relative delay between signal and reference, and the correlation peak amplitude was again shown to vary linearly with input signal duration, Fig. 6. Further measurements have been made for 2.5 mS and 10 mS integration periods. Here the correlation peak amplitude at maximum integration time was essentially identical to the previous 1 mS result, as was shown previously in the upper curve of Fig. 2.

IV. SAW Storage Correlator Application in Adaptive Filtering

This section describes a new realization of adaptive transversal filter or equalizer[9] based on the storage correlator. It operates by storing directly a sample of the input signal to implement a narrowband filter, which is subsequently used to suppress narrowband interference in a simulated spread spectrum receiver. These receivers often experience very high levels of interference, which prevent demodulation of the received message even

after matched filter processing. Wideband interference is suppressed by spatial processing in an adaptive array[9] while narrowband interference can be suppressed in an adaptive transversal filter.

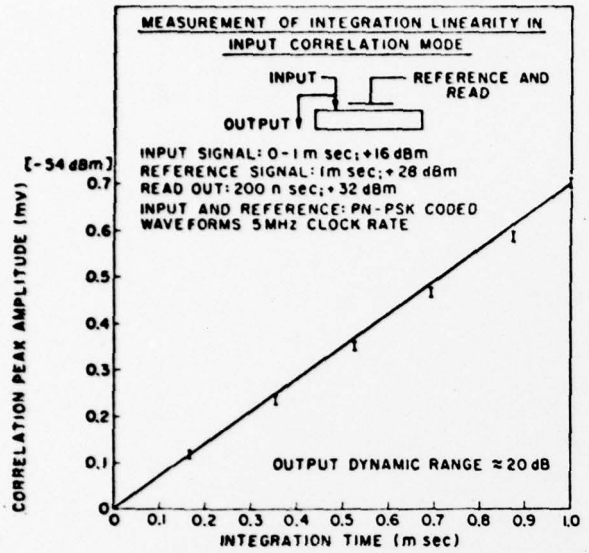

FIGURE 6. Measurement of device linearity with input signal duration.

One possible implementation of this latter processor is shown in Fig. 7. Here a programmable notch filter is realized by loading and storing a sample of the input signal in a SAW correlator. As the narrowband CW interference is considerably larger than the wideband coded signal, the correlator impulse response comprises a burst of CW whose duration equals the delay across the semiconductor interaction region. Thus it implements a filter with a narrowband (sin x)/x frequency response which is automatically set on the interfering frequency. When incorporated as in Fig. 7, the SAW device outputs only the interfering signal which is subsequently amplified to overcome the loss in the filter and added in antiphase with the input signal. This implements a wideband filter with a notch centered on the interference frequency.

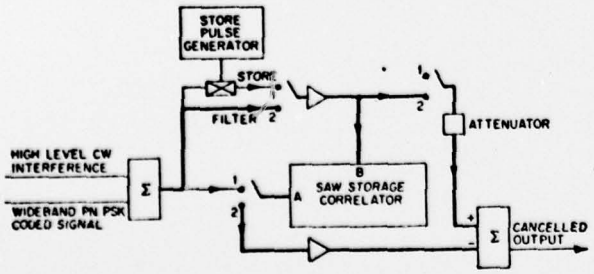

FIGURE 7. SAW implementation of narrowband interference canceller.

The test scheme adopted for the practical verification of the adaptive filter is detailed in Fig. 7. Here the switches are set in position 1 for signal storage while the adaptive filter operation is performed in position 2, where the bold lines show the signal path. We have previously[10] utilized a short (< 1μS) gated burst of CW to energize the storage diodes and have shown that it permits the filter to notch out interference signals by -20 dB when used with burst PN-PSK coded spread spectrum signals.

Figure 8 shows more recent results, which have been obtained with a continuous PN-PSK spread spectrum coded signal, by storing with input correlation techniques. The upper trace shows the signal input to our SAW based adaptive processor. It comprises a +10 dBm, 120.9 MHz CW signal plus a -20 dB 31 chip PN code, modulated at 5 MHz rate onto a 120 MHz carrier. The direct correlation of this composite signal in a 31 chip matched filter, without the adaptive processor, is shown in trace (b). For adaptive filter operation, the input signal was stored in the correlator by input correlation, by amplifying the input to +20 dBm and applying it to the top plate. Cancellation was achieved by summing the +40 dB amplified filter output with the 30 dB attenuated input after ensuring that the signals are arranged in antiphase. This implements a flat amplitude characteristic filter with a single notch at the interference frequency. This correlator, which stored a T = 3 μS signal sample, realized a 30 dB deep notch whose width was approximately 330 kHz corresponding to

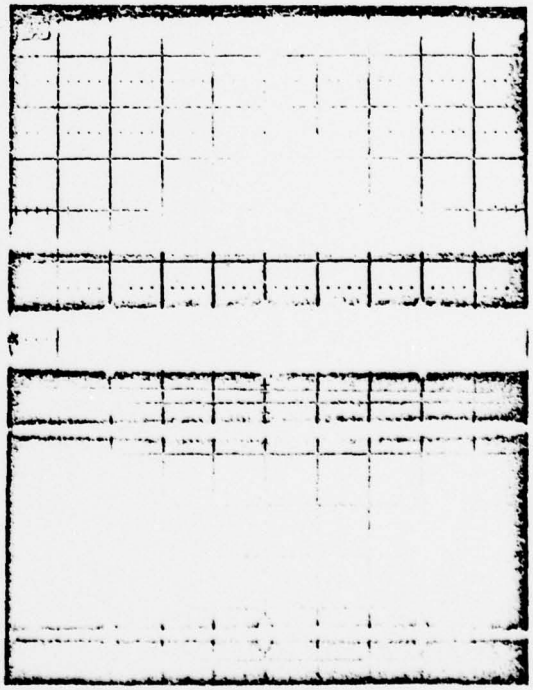

FIGURE 8. SAW adaptive filter demonstration. Scale 2 μS per division.

the reciprocal of the device transit time (3 μsec). A comparison between the input signal trace (a) and the cancelled output signal, trace (c), clearly shows the 30 dB suppression of the 120.9 MHz interference, leaving the wideband coded signal just visible. The adaptive interference canceller permitted the correlation peak from the final matched filter to be clearly detected, trace (d). We have also shown that after our processor is set up and optimized it can simultaneously notch out one or more interfering frequencies anywhere within the 8 MHz bandwidth of our SAW storage correlator. This capability is achieved as the cancelling signal from the filter and the input signal are always in antiphase with our storage arrangement.

V. Conclusions

This paper has presented new results on the operation of the SAW storage correlator in input correlation mode which show exceptional linearity between the input and output ports, with varying input power levels. It is extremely encouraging to obtain these excellent results as it appears that this mode, which offers the realization of very large correlator time bandwidth product, will be potentially most useful for signal processing. The application of the device for correlation of large TB product (5,000) PN-PSK coded waveform and adaptive filtering for the suppression by 30 dB of a narrowband jamming signal has also been demonstrated. It is in the latter area of adaptive filtering that we believe the wideband storage correlator will be most significant both for equalization in communications and inverse filtering in radar and acoustic imaging systems.

Acknowledgement

This work was supported by the Defense Advanced Research Projects Agency and monitored by the Office of Naval Research under Contract N00014-76-C-0129.

References

1. P. C. Borden and G. S. Kino, "An Analytic Theory for the Storage Correlator," 1977 IEEE Ultrasonic Symposium Proceedings, pp. 485-491.

2. H. C. Tuan, B. T. Khuri-Yakub, and G. S. Kino, "A New Zinc-Oxide-on-Silicon Monolithic Storage Correlator," 1977 IEEE Ultrasonics Symposium Proceedings, pp. 496-499.

3. P. R. Emtage, Private Communication.

4. R. W. Ralston, D. H. Hurlburt, F. J. Leonkerger, J. H. Cafarella, and E. Stern, "A New Signal-Processing Device, the Integrating Correlator," 1977 IEEE Ultrasonics Symposium Proceedings, pp. 623-628.

5. R. W. Ralston, Private Communication.

6. J. H. Collins, P. M. Grant, and B. J. Darby, "Application of SAW Devices to Spread Spectrum Communications," Wave Electronics 1 No. 5/6, pp. 311-342 (June 1976).

7. J. M. Hannan, et al., "Code Synchronization System Using Cascaded SAW Convolvers," Paper K3 this conference.

8. D. P. Morgan, et al., "Spread Spectrum Synchronization Using a SAW Convolver and Recirculating Loop," Proc. IEEE 64, #5, pp. 751-753 (May 1976).

9. B. Widrow, et al., "Adaptive Noise Cancellation: Principles and Applications," Proc. IEEE 63, #12, pp. 1692-1716 (1975).

10. P. M. Grant and G. S. Kino, "Adaptive Filter Based on SAW Monolithic Storage Correlator," to be published in Electronics Letters (1978).